Bulletin of the Seismological Society of America. Vol. 65, No. 3, pp. 581–626. June 1975

A STUDY ON THE DURATION OF STRONG EARTHQUAKE GROUND MOTION

BY M. D. TRIFUNAC AND A. G. BRADY

A simple definition of the duration of strong earthquake ground motion based on the mean-square integral of motion has been presented. It is closely related to that part of the strong motion which contributes significantly to the seismic energy as recorded at a point and to the related spectral amplitudes. Correlations have been established between the duration of strong-motion acceleration, velocity, and displacement and Modified Mercalli intensity, earthquake magnitude, the type of recording site geology, and epicentral distance. Simple relations have been presented that predict the average trend of the duration and other related parameters as a function of Modified Mercalli intensity, earthquake magnitude, site geology and epicentral distance.

INTRODUCTION

The duration of strong earthquake ground motion is one of the main parameters characterizing this natural phenomenon. Yet very little has been done, so far, to describe it quantitatively in terms of earthquake magnitude, source-to-station distance and the effects of geological environment. Remembering the significance of the duration of excitation on the response of nonlinear yielding structures and that it determines the number of cycles during vibration, it becomes evident that, together with the overall amplitudes of induced response, the duration must play a major role in governing the outcome of any response to strong earthquake shaking. Recent model studies of the response of simple yielding structures to earthquake-like excitation have indicated the full significance of the duration of ground shaking on the computed response (e.g., Husid, 1967).

Several important contributions to the description of the duration of strong earthquake ground motion were, for example, those of Esteva and Rosenblueth (1964), Housner (1965) and Bolt (1973). Esteva and Rosenblueth describe the duration, s(sec) of an equivalent ground motion with uniform intensity per unit time by

$$s = 0.02 \exp(0.74M) + 0.3\Delta \tag{1}$$

where M is earthquake magnitude and Δ(km) is the source-to-station distance. Using 16 measurements and several witnesses' reports on the duration of shaking during large earthquakes, Housner (1965) proposed an upper bound for the duration, D(sec), of ground motion. This upper bound is approximated by a linear law of the form

$$D = 11.2M - 53, \quad \text{for } M > 5. \tag{2}$$

For large earthquakes, $M = 8.5^{+}$, this bound yields a maximum duration of about 45 sec. The results of Bolt (1973) for the "bracketed duration" of acceleration greater than 0.05 g are essentially the same as those of Housner (1965).

The major difficulty in studying the duration of strong earthquake ground motion results from the fact that it is not obvious how to define duration in the most general yet useful way. For structural response calculations it would be ideal to develop a definition of duration that would be frequency-dependent. Since the approximate law of seismic-

wave attenuation incorporates the factor $\exp(-\pi\Delta/TQc)$, where Δ is the source-to-station distance, T is the period of wave motion, Q is the attenuation constant and c is the respective wave velocity, the effective duration for short-period oscillations is obviously less than for longer period oscillations. Another important consideration in defining the duration of strong ground motion is the question of which sections of the record should be included in the final estimate of duration. Should one take a time interval between the first and last times that the acceleration, velocity, or displacement exceeds some preselected amplitude? Or, perhaps, should one add together only those time intervals during which the acceleration, velocity, or displacement exceeds some level? It seems now that several different definitions of the duration of strong ground motion may eventually be called for in accordance with the specific requirements of design practice.

The purpose of this paper is to present the average and overall trends and correlations of the duration of strong earthquake ground motion with Modified Mercalli intensity, earthquake magnitude, source-to-station distance, and site conditions. The simple methods and definitions used for these correlations will be based on the spectral energy content. Although this may not represent the most direct way of presenting such correlations to the earthquake engineering community, it seems that the methods used in our study provide an adequate basis for the approximate description of the duration of strong ground shaking and other related quantities.

Some Definitions and Assumptions

The differential equation of relative motion $x(t)$ of a single-degree-of-freedom oscillator with natural frequency ω_n and fraction of critical damping, ζ, is

$$\ddot{x}+2\omega_n\zeta\dot{x}+\omega_n{}^2x = a \tag{3}$$

where a is the negative absolute acceleration of its support.

Suppose we want to calculate the work per unit mass done by the inertial force term $\ddot{x}$, dash-pot term $2\omega_n\zeta\dot{x}$, and the elastic spring term $\omega_n{}^2x$ throughout the entire excitation and for all oscillators with frequencies ω_n between 0 and ∞. This would be obtained by evaluating the following integral

$$I = \int_0^\infty \int_0^\infty a(t)\dot{x}(t)\,dt\,d\omega_n. \tag{4}$$

Interchanging the order of integration and noting that

$$\int_0^\infty \dot{x}(t)\,d\omega_n = a(t)\,\frac{\cos^{-1}\zeta}{\sqrt{1-\zeta^2}} \tag{5}$$

we get

$$I = \frac{\cos^{-1}\zeta}{\sqrt{1-\zeta^2}}\int_0^\infty [a(t)]^2\,dt. \tag{6}$$

This result is analogous to that derived by Arias (1970) for a "Measure of Earthquake Intensity."

Next suppose that we want to calculate the seismic-wave energy, E_s, radiated from an earthquake source, using the recorded ground motion at some point away from the source. The formula we would use in such a calculation would, of course, depend on the type of waves that have been recorded and on the degree of sophistication employed in our analysis. It could be of the following form

$$E_s = \Psi(\text{Instr., } Q, \Delta, \text{S.M.}) \int_0^\infty v^2(t)\,dt \tag{7}$$

where $\Psi(\cdot)$ is some function of the instrument used for recording, attenuation constant Q, source-to-station distance Δ, and the source mechanism, as well as its radiation pattern (Wu, 1966).

In the statistics of peak amplitudes of random functions that can be used to study the peaks of strong ground motion, $a_{\max}$, $v_{\max}$, and $d_{\max}$, the following expressions are frequently encountered

$$E\begin{Bmatrix} a_{\max} \\ v_{\max} \\ d_{\max} \end{Bmatrix} = \phi\left[N\begin{pmatrix} a \\ v \\ d \end{pmatrix}, \varepsilon\begin{pmatrix} a \\ v \\ d \end{pmatrix}\right] \begin{Bmatrix} \frac{1}{T}\left(\int_0^T a^2\,dt\right)^{1/2} \\ \frac{1}{T}\left(\int_0^T v^2\,dt\right)^{1/2} \\ \frac{1}{T}\left(\int_0^T d^2\,dt\right)^{1/2} \end{Bmatrix}. \tag{8}$$

Here $E(\cdot)$ represents the expected value of $a_{\max}$, $v_{\max}$, or $d_{\max}$, ϕ is a function that depends on the number of peaks of the entire time history of $a(t)$, $v(t)$, or $d(t)$ and ε measures the spectral width of the power spectra of $a(t)$, $v(t)$, or $d(t)$ (Udwadia and Trifunac, 1974).

Although the three formulations summarized in expressions (6), (7), and (8) are physically completely unrelated, the equations do have one common feature, an integral of the form $\int_0^T f^2(t)\,dt$, where $f(t)$ stands for acceleration $a(t)$, velocity $v(t)$, or displacement $d(t)$ and T is finite or infinite. The nature of growth of these integrals is shown in Figure 1 for typical acceleration, velocity, and displacement curves. It is seen from this figure that the integrals $\int_0^T a^2\,dt$, $\int_0^T v^2\,dt$, and $\int_0^T d^2\,dt$ increase rapidly at first, and then tend asymptotically toward their final amplitudes $\int_0^\infty a^2\,dt$, $\int_0^\infty v^2\,dt$, and $\int_0^\infty d^2\,dt$. Detailed study of many such integrals shows that the rapid growth corresponds to the "strong motion" part of the recorded ground vibrations and that it is associated with essentially all seismic-wave energy recorded at a station. The subsequent interval of time during

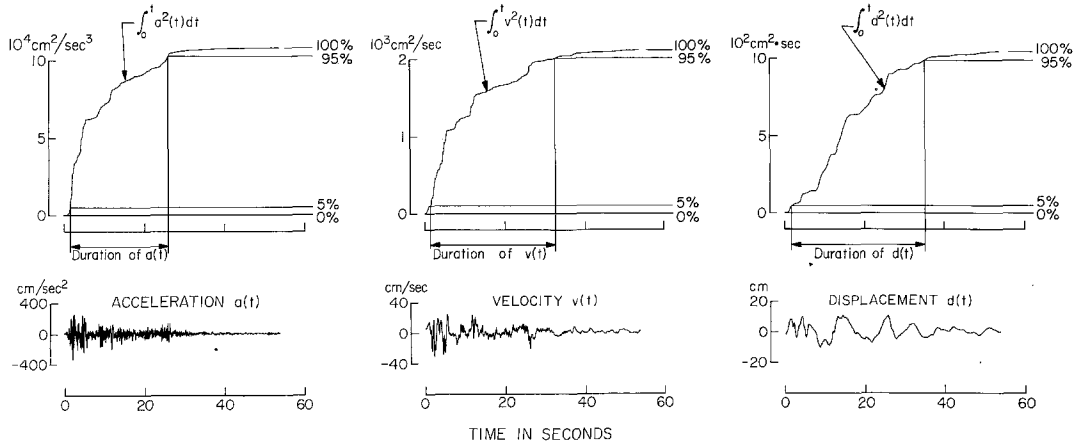

FIG. 1. Estimation of duration of acceleration, velocity, and displacement for a typical record (south component of El Centro, May 18, 1940).

which these integrals gradually approach their final amplitudes results from the late arrivals of scattered, diffracted, and other coda waves that travel along longer and indirect paths, suffer more pronounced attenuation and thus contribute only minor additional energy to the complete signal. Based on these observations we propose to define the duration of the recorded strong ground motion to be that time interval during

TABLE 1
SUMMARY OF 188 ACCELEROGRAMS USED IN THIS STUDY

Earthquake Location	Date	Time	Caltech I.D. No.*
Long Beach, Calif.	3/10/33	1754 PST	B021, V314, V315
Southern Calif.	10/02/33	0110 PST	B023
Eureka, Calif.	7/06/34	1449 PST	U294
Lower Calif.	12/30/34	0552 PST	B024
Helena, Montana	10/31/35	1138 MST	B025
Helena, Montana	11/31/35	1218 MST	U295
Helena, Montana	11/28/35	0724 MST	U297 (9 sec)†
Humboldt Bay, Calif.	2/06/37	2042 PST	U298
Northwest Calif.	9/11/38	2210 PST	B026
Imperial Valley, Calif.	5/18/40	2037 PST	A001
Northwest Calif.	2/09/41	0145 PST	B027
Santa Barbara, Calif.	6/30/41	2351 PST	U299
Northern Calif.	10/03/41	0813 PST	U300
Torrance-Gardena, Calif.	11/14/41	0042 PST	V316, V317
Borrego Valley, Calif.	10/21/42	0822 PST	T286
Northern Calif.	3/09/49	0429 PST	U301
Western Washington	4/13/49	1156 PST	B028, B029
Imperial Valley, Calif.	1/23/51	2317 PST	T287
Northwest Calif.	10/07/51	2011 PST	A002
Kern County, Calif.	7/21/52	0453 PDT	A003, A004, A005, A006, A007
Northern Calif.	9/22/52	0441 PDT	B030
Southern Calif.	11/21/52	2346 PST	V319
Imperial Valley, Calif.	6/13/53	2017 PST	T288
Wheeler Ridge, Calif.	1/12/54	1534 PST	B031
Central Calif.	4/25/54	1233 PST	U305
Lower Calif.	11/12/54	0427 PST	T289
Eureka, Calif.	12/21/54	1156 PST	A008, A009
San Jose, Calif.	9/04/55	1801 PST	A010
Imperial County, Calif.	12/16/55	2207 PST	T292
El Alamo, Baja Calif.	2/09/56	0633 PST	A011
Southern Calif.	3/18/57	1056 PST	V329
San Francisco, Calif.	3/22/57	1048 PST	V320
San Francisco, Calif.	3/22/57	1144 PST	A013 (25 sec), A014 (26 sec), A015 (27 sec), A016 (25 sec), A017
San Francisco, Calif	3/22/57	1515 PST	V322, V323
San Francisco, Calif.	3/22/57	1627 PST	V328
Central Calif.	1/19/60	1926 PST	U307
Northern Calif.	6/05/60	1718 PST	U308
Hollister, Calif.	4/08/61	2323 PST	A018, U309
Northern Calif.	9/04/62	0917 PST	V330 (75 sec)
Puget Sound, Washington	4/29/65	0729 PST	B032, U310
Southern Calif.	7/15/65	2346 PST	V331
Parkfield, Calif.	6/27/66	2026 PST	B033, B034, B035, B036, B037, B038, U311
Gulf of Calif.	8/07/66	0936 PST	T293
Northern Calif.	9/12/66	0841 PST	V332
Northern Calif.	12/10/67	0407 PST	B039, U312
Northern Calif.	12/18/67	0925 PST	U313
Borrego Mtn., Calif.	4/08/68	1830 PST	A019, A020, B040, Y370, Y371, Y372, Y373, Y375, Y376, Y377, Y378, Y379, Y380

TABLE 1—*continued*

Earthquake Location	Date	Time	Caltech I.D. No.*
Lytle Creek, Calif.	9/12/70	0630 PST	W334, W335, W336, W338, W339, W342, W344
San Fernando, Calif.	2/09/71	0600 PST	C041 (31 sec), C048, C051, C054, D056, D057, D058, D059, D062, D065, D068, E071, E072, E075, E078, E081, E083, F086, F087, F088 (30 sec), F089, F092, F095, F098, F101, F102, F103, F104, F105, G106 (31 sec), G107, G108, G110, G112, G114, H115, H118, H121, H124, I128, I131, I134, I137, J141, J142, J143, J144, J145, J148, K157 (32 sec), L166, L171, M176, M179, M180, M183, M184, N185, N186, N187, N188, N191, N192, N195, N196, N197, O198 (31 sec), O199 (35 sec), O204, O205, O206, O207, O208, O210, O213, P214 (30 sec), P217 (30 sec), P220, P221, P222, P223, P231, Q233, Q236, Q239, Q241, R244, R246, R248, R249, R251 (31 sec), R253, S255 (30 sec), S258, S261, S262, S265, S266 (35 sec), S267			

*Hudson, *et al.* (1971).

†Record numbers with a record length in parentheses have been shortened to this length in order to eliminate aftershocks.

which the most significant contribution to these integrals takes place. For definiteness, but quite arbitrarily, we delete the first 5 per cent and the last 5 per cent amplitudes of these integrals and define the remaining 90 per cent as the "significant" or "strong-motion" contribution. Consequently, the time interval remaining between the low and the high 5 per cent cut-offs becomes the "duration" of strong ground motion (Figure 1).

Recalling Parseval's theorem, which states that

$$\int_{-\infty}^{\infty} f^2(t)\,dt = \frac{1}{2\pi}\int_{-\infty}^{\infty} |F(\omega)|^2\,d\omega \tag{9a}$$

where

$$F(\omega) = \textstyle\int_{-\infty}^{\infty} f(t)\exp(-i\omega t)\,dt, \tag{9b}$$

we observe that the above integrals are also closely related to the integrals of response spectra (Udwadia and Trifunac, 1973; 1974) which have been used to define the spectral intensity of earthquakes (e.g., Housner, 1952). Therefore, if one were to calculate response spectra only from the "strong-motion" part of an accelerogram using the above definition of duration, one would obtain results which would, on the average, be about 90 per cent of those computed from the complete length of the accelerograms.

Having computed the integrals of the form $\int_0^{\infty} f^2(t)\,dt$ and the duration of strong ground motion, we can next compute the average rate at which the seismic-wave energy passes by a recording station. This quantity, which is proportional to the rate as defined by

$$\text{Rate} \equiv \left(\textstyle\int_0^{\infty} f^2(t)\,dt\right)/\text{duration}, \tag{10}$$

may also be useful in structural response calculations. Whether in the linear domain with viscous damping, or in the nonlinear range of response, a particular structure can dissipate only a certain amount of vibrational energy per unit time. If it should be possible to maintain this dissipation rate higher than the rate of the input seismic energy, it would indicate that the structure might successfully survive that particular excitation. Conversely, if the input rate should be higher, the structure might experience permanent progressive damage to create a higher energy dissipation capacity, and if shaking should continue, it would eventually collapse. We note here that the "rate" as we defined it in (10) is only proportional to the actual rate at which energy is fed into the structure. The constant of

proportionality depends on the type of waves which dominate the strong ground motion and on the soil-structure interaction mechanism of the particular structure.

It should be noted here that the "rate" as defined by equation (10) is proportional to $\overline{f^2}$, the mean-square value of $f(t)$, evaluated over the duration described above. Since

$$\overline{f^2} \equiv \frac{1}{T_2 - T_1} \int_{T_1}^{T_2} f^2(t)\,dt \tag{11}$$

is evaluated over the interval T_1 to T_2, we can choose the interval to be the duration. In this case, using equation (10), and the fact that $f(t)$ is assumed zero for t greater than the record length T, we have

$$\overline{f^2} = 0.9 \text{ Rate}.$$

Strong-Motion Data, Site Classification, and Strategy of this Paper

Table 1 lists 188 acceleration records (563 components) used in this study. For some longer records, when the digitized versions contained one or more aftershocks, the digitized records were shortened to include only the main earthquake. These shortened records are indicated in Table 1. We restrict the investigations here to records of strong ground motion within the frequency band of 0.07 to 25.0 Hz (Hudson, *et al.*, 1971). Peak amplitudes of these strong-motion records are in general at least 0.05 *g*.

The site classification employed in this work is identical to that presented in our previous paper (Trifunac and Brady, 1975). All accelerograph stations that recorded on alluvium or otherwise "soft" sedimentary deposits have been classified under 0. The sites located on "hard" basement rocks were labeled by 2, whereas the sites located on "intermediate" type rocks or in a complex environment which could not be identified as either 0 or 2 have all been grouped under 1.

We begin by considering correlations of the integrals of the form $\int_0^\infty f^2(t)\,dt$, where $f(t)$ can stand for acceleration, velocity, or displacement, with Modified Mercalli intensity, earthquake magnitude, site conditions, and epicentral distance. Having developed these correlations, we examine how the duration of strong-motion acceleration, velocity, and displacement depends on the same quantities. Finally, we develop similar correlations for the rate of growth of strong ground motion.

Unless stated otherwise, the units in this paper will be centimeters and seconds for acceleration, velocity, and displacement, seconds for duration, and kilometers for epicentral distance.

Correlations of Basic Integrals with the Modified Mercalli Intensity and Site Classifications

It is well known that the Modified Mercalli intensity scale represents only a qualitative measure of intensity of strong ground motion. Its descriptive nature is based on the subjective assessment of vibration and damage as characterized by the people who experienced the shaking. However, since the Modified Mercalli intensity or its equivalent represent the only information available for the classification of earthquakes prior to the beginning of the 20th century, it is essential to "calibrate" the Modified Mercalli intensity scale through correlations with a broad class of instrumental measurements. Such correlations will help not only in the comparison of different methods of intensity ratings in different countries, but also should provide means for more meaningful assessment and description of levels of shaking during earthquakes that occurred before the development

of instrumental seismology. Since the above integrals enter as scaling factors into numerous measures of strong ground motion [e.g., equations (6), (7) and (8)], it is useful to find how they correlate with the Modified Mercalli intensity.

Table 2 and Figure 2 (a, b, and c) present those correlations for vertical and horizontal components of ground motion. As may be seen from Table 2, an adequate number of data points is available only for intensities V, VI and VII. Nevertheless, in Figure 2 (a, b, and c) we present all available information in an attempt to define the overall trend of data.

TABLE 2

CORRELATION OF $\int_0^T a^2dt$, $\int_0^T v^2dt$, AND $\int_0^T d^2dt$ WITH MODIFIED MERCALLI INTENSITY

Intensity	Component	$\log_{10}(\int a^2dt)$		$\log_{10}(\int v^2dt)$		$\log_{10}(\int d^2dt)$		No. of Data
		Mean	Standard deviation	Mean	Standard deviation	Mean	Standard deviation	
III	Vertical	1.10	0.30	0.70	0.40	1.10	0.40	2
	Horizontal	1.25	1.05	0.40	1.00	0.40	1.11	4
IV	Vertical	2.10	0.16	0.97	0.25	1.30	0.16	3
	Horizontal	2.67	0.27	1.27	0.27	1.27	0.21	6
V	Vertical	2.43	0.69	0.93	0.62	0.89	0.64	34
	Horizontal	2.85	0.77	1.22	0.74	1.04	0.70	68
VI	Vertical	2.79	0.63	1.36	0.61	1.25	0.54	66
	Horizontal	3.41	0.63	1.89	0.68	1.65	0.71	132
VII	Vertical	3.56	0.46	2.01	0.58	1.63	0.50	76
	Horizontal	4.10	0.46	2.62	0.67	2.21	0.66	151*
VIII	Vertical	3.77	0.55	1.97	0.62	2.00	0.75	6
	Horizontal	4.37	0.43	2.65	0.52	2.33	0.72	12
X	Vertical	5.30	—	3.30	—	3.10	—	1
	Horizontal	5.70	—	3.70	0.20	3.00	0.50	2

*Record B033 recorded during Parkfield, California, earthquake of 1966 had only one horizontal and vertical component suitable for analysis. The other horizontal transducer malfunctioned and left no acceleration trace.

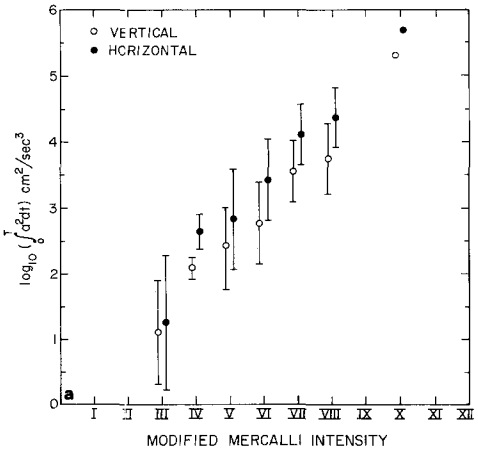

FIG. 2a. Mean values and standard deviations of the integral $\int_0^T a^2dt$ for horizontal and vertical components at different Modified Mercalli intensities.

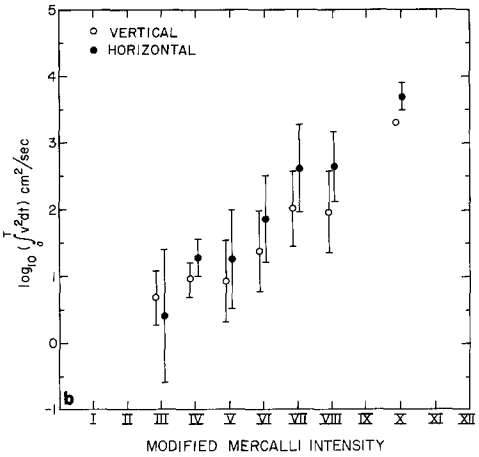

FIG. 2b. Mean values and standard deviations of the integral $\int_0^T v^2 dt$ for horizontal and vertical components at different Modified Mercalli intensities.

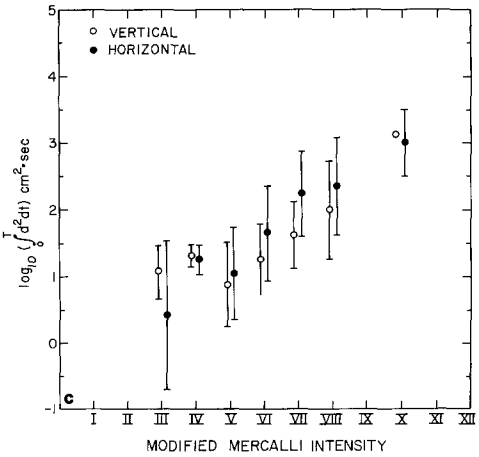

FIG. 2c. Mean values and standard deviations of the integral $\int_0^T d^2 dt$ for horizontal and vertical components at different Modified Mercalli intensities.

Detailed analysis of Figure 2 (a, b, and c) shows slight curvature and leveling off in Figure 2 (b and c) for Modified Mercalli intensities less than about V and could be attributed to a contribution of noise in those digitized accelerograms which are characterized by low acceleration amplitudes (Trifunac and Brady, 1975). This effect is more pronounced for velocity and displacement integrals since the successive integration of ground acceleration emphasizes the low-frequency noise amplitudes which are characterized by a low signal-to-noise ratio. If one neglects these deviations for intensities less than V, it appears that the logarithms of $\int_0^T a^2 dt$, $\int_0^T v^2 dt$ and $\int_0^T d^2 dt$ scale approximately in a linear manner with the Modified Mercalli intensity as follows

$$\log_{10}\left(\int_0^T a^2 dt\right) = \begin{Bmatrix} 0.72 + 0.47\ I_{MM} \text{ for horizontal accelerations} \\ 0.25 + 0.45\ I_{MM} \text{ for vertical accelerations} \end{Bmatrix} \quad \text{for III} \leqq I_{MM} \leqq \text{VIII} \tag{12}$$

$$\log_{10}\left(\int_0^T v^2 dt\right) = \begin{Bmatrix} -0.96 + 0.47\ I_{MM} \text{ for horizontal velocities} \\ -0.90 + 0.38\ I_{MM} \text{ for vertical velocities} \end{Bmatrix} \quad \text{for V} \leqq I_{MM} \leqq \text{VIII} \tag{13}$$

and

$$\log_{10}\left(\int_0^T d^2\,dt\right) = \begin{cases} -1.10+0.45\ I_{MM} \text{ for horizontal displacements} \\ -0.97+0.37\ I_{MM} \text{ for vertical displacements} \end{cases} \quad (14)$$
$$\text{for } V \leqq I_{MM} \leqq VIII.$$

It should be noted here that these correlations represent only preliminary approximate trends and that the coefficients in these equations should be revised when more complete and accurate strong-motion data becomes available. This remark applies, of course, to all other similar correlations presented in this paper.

One standard deviation for the above correlations is about 0.6 on the logarithmic scale (Table 2). Although this represents a smaller scatter of data than the scatter in correlations of peak acceleration, peak velocity, and peak displacement with the Modified Mercalli intensity (Trifunac and Brady, 1975), it is larger than what one might suppose knowing that the integration represents a smoothing operation.

The effect of site conditions on the correlations between the $\log_{10}\left(\int_0^T a^2\,dt\right)$, $\log_{10}\left(\int_0^T v^2\,dt\right)$, and $\log_{10}\left(\int_0^T d^2\,dt\right)$ and the Modified Mercalli intensity are presented in Figure 3 (a, b, and c) and in Table 3. For sites on "soft" alluvium deposits the averages of

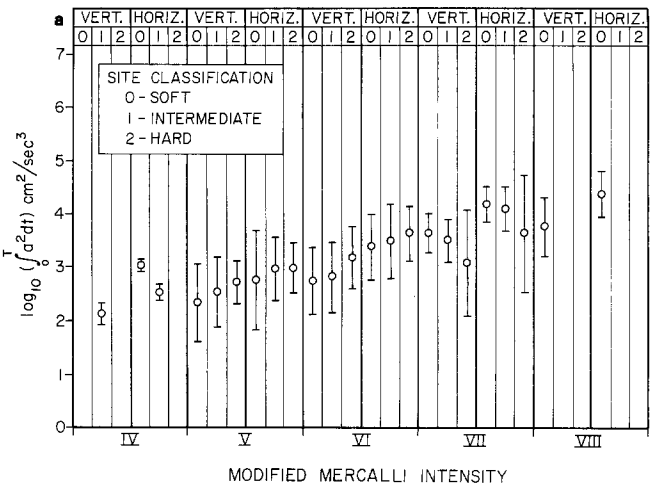

FIG. 3a. Mean values and standard deviations of the integral $\int_0^T a^2\,dt$ for horizontal and vertical components at different site conditions and Modified Mercalli intensities.

$\int_0^T v^2\,dt$ and $\int_0^T d^2\,dt$ are larger by a factor of 2 to 10 when compared with those classified under 2. The factor of about 2 is typical for small intensities, while the factor of 10 and more characterizes higher intensity levels. For $\int_0^T a^2\,dt$ this general trend is reversed for intensities smaller than VII where we observe the average of $\int_0^T a^2\,dt$ on "hard" sites about twice larger than those on the "soft" alluvium deposits. Detailed explanation of these trends is beyond the scope of this paper and will have to await more abundant data, especially for low and high intensities. Qualitatively, however, these trends in Figure 3a may be explained by the attenuation of high-frequency waves at greater distances where $\exp(-\omega\Delta/2Qc)$ attenuates more effectively than soft alluvial deposits can amplify the incident waves. The large mean values of $\int_0^T v^2\,dt$ and $\int_0^T d^2\,dt$ recorded on "soft" alluvium appear to be caused by longer duration of shaking there. Since the overall amplitude amplification of $v(t)$ and $d(t)$ for 0 site conditions is only about two times the average amplitude recorded on "hard" rocks (Trifunac and Brady, 1975), the only way for $\int_0^T v^2\,dt$ and $\int_0^T d^2\,dt$ to increase by a factor of about 10 is to have the duration at a site of

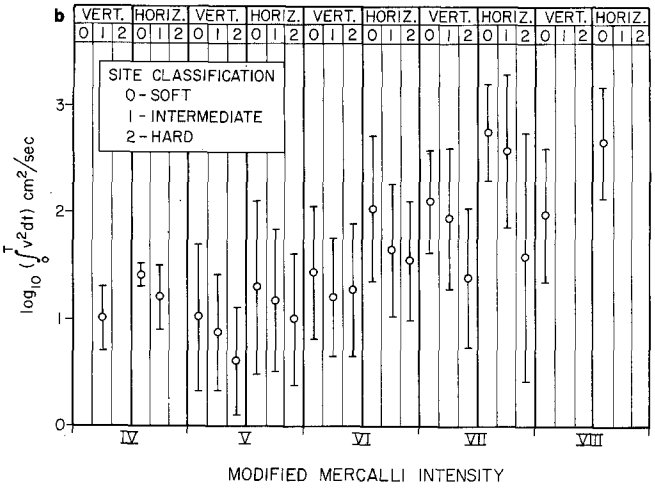

FIG. 3b. Mean values and standard deviations of the integral $\int_0^T v^2 dt$ for horizontal and vertical velocities at different site conditions and Modified Mercalli intensities.

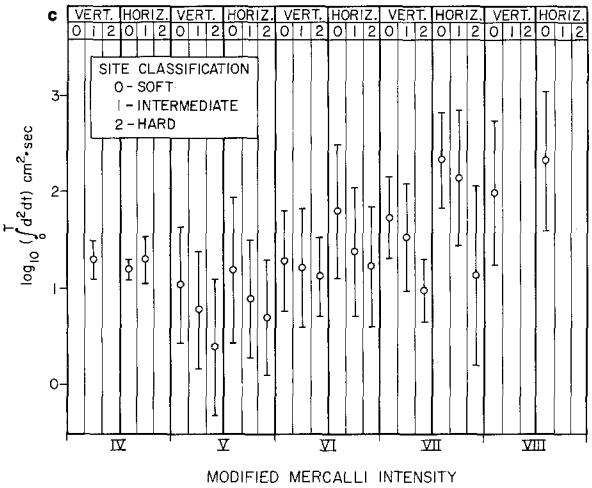

FIG. 3c. Mean values and standard deviations of the integral $\int_0^T d^2\, dt$ for horizontal and vertical displacements at different site conditions and Modified Mercalli intensities.

class 0 be about 2 to 3 times the duration at a site of class 2. It will be seen from what follows that this seems to be so.

CORRELATIONS OF BASIC INTEGRALS WITH EARTHQUAKE MAGNITUDE, EPICENTRAL DISTANCE, AND SITE CLASSIFICATION

The correlations of $\int_0^T a^2 dt$, $\int_0^T v^2 dt$, and $\int_0^T d^2 dt$ with site classifications 0, 1 and 2, earthquake magnitude, M, and the epicentral distance Δ should be valuable for the development of theoretical models that specify the shape of the response and Fourier spectra of acceleration, velocity, and displacement in terms of these same parameters. The functional form of such correlations is not known at this time, and it may be difficult to derive it empirically because of the limited number of data points available within the narrow magnitude and distance intervals. Furthermore, the available data are not uniformly distributed between site classifications 0, 1, and 2, because most of the record-

TABLE 3

CORRELATION OF $\int_0^T a^2dt$, $\int_0^T v^2dt$, AND $\int_0^T d^2dt$ WITH MODIFIED MERCALLI INTENSITY AND DIFFERENT (0, 1 AND 2) SITE CONDITIONS

Intensity	Component	$\log_{10}(\int_0^T a^2dt)$		$\log_{10}(\int_0^T v^2dt)$		$\log_{10}(\int_0^T d^2dt)$		No. of Data
		Mean	Standard deviation	Mean	Standard deviation	Mean	Standard deviation	
III–0	Vertical	1.90	—	1.10	—	1.50	—	1
	Horizontal	2.30	—	1.40	0.10	1.50	0.20	2
III–1	Vertical							
	Horizontal							
III–2	Vertical	0.30	—	0.30	—	0.70	—	1
	Horizontal	0.20	0.10	−0.60	0.10	−0.70	—	2
IV–0	Vertical	2.10	—	0.90	—	1.30	—	1
	Horizontal	3.00	0.10	1.40	0.10	1.20	0.10	2
IV–1	Vertical	2.10	0.20	1.00	0.30	1.30	0.20	2
	Horizontal	2.50	0.14	1.20	0.30	1.30	0.24	4
IV–2	Vertical							
	Horizontal							
V–0	Vertical	2.32	0.73	1.02	0.68	1.04	0.60	17
	Horizontal	2.75	0.92	1.29	0.81	1.19	0.75	34
V–1	Vertical	2.51	0.65	0.87	0.54	0.79	0.61	15
	Horizontal	2.95	0.59	1.17	0.66	0.90	0.61	30
V–2	Vertical	2.70	0.40	0.60	0.50	0.40	0.70	2
	Horizontal	2.95	0.46	1.00	0.61	0.70	0.60	4
VI–0	Vertical	2.73	0.62	1.43	0.62	1.29	0.52	43
	Horizontal	3.36	0.61	2.03	0.68	1.81	0.69	86
VI–1	Vertical	2.80	0.64	1.20	0.55	1.21	0.61	16
	Horizontal	3.47	0.70	1.64	0.62	1.39	0.66	32
VI–2	Vertical	3.16	0.58	1.27	0.62	1.13	0.41	7
	Horizontal	3.63	0.52	1.54	0.56	1.24	0.62	14
VII–0	Vertical	3.64	0.36	2.10	0.48	1.74	0.42	50
	Horizontal	4.16	0.32	2.75	0.45	2.34	0.49	99*
VII–1	Vertical	3.49	0.40	1.95	0.66	1.54	0.55	21
	Horizontal	4.07	0.41	2.57	0.72	2.15	0.70	42
VII–2	Vertical	3.06	1.00	1.38	0.65	0.98	0.32	5
	Horizontal	3.64	1.10	1.58	1.16	1.14	0.93	10
VIII–0	Vertical	3.77	0.55	1.97	0.62	2.00	0.75	6
	Horizontal	4.37	0.43	2.65	0.52	2.33	0.72	12
VIII–1	Vertical							
	Horizontal							
VIII–2	Vertical							
	Horizontal							
X–0	Vertical							
	Horizontal							
X–1	Vertical							
	Horizontal							
X–2	Vertical	5.30	—	3.30	—	3.10	—	1
	Horizontal	5.70	—	3.70	0.20	3.00	0.50	2

*See footnote to Table 2.

ings were made on "soft" alluvium. For these reasons, we consider only the simplest type of linear regression of the form

$$\log_{10}\left\{\int_0^T \begin{pmatrix} a^2 \\ v^2 \\ d^2 \end{pmatrix} dt\right\} = as+bM+c\log_{10}\Delta+d\pm\sigma, \tag{15}$$

where s stands for site classification and takes on values 0, 1 or 2, M is earthquake magnitude, Δ is epicentral distance and a, b, c, and d are correlation coefficients.

The coefficients in equation (15) have been determined from 181 data points for vertical components and 362 data points for horizontal components [Figure 4 (a to f)] by using a least-squares fit. The regression coefficients thus obtained are given in Table 4. In agreement with Figure 3 (a, b, and c) the coefficients a in Table 4 indicate more pronounced influence of site classification on $\int_0^T v^2\,dt$ and $\int_0^T d^2\,dt$ than for $\int_0^T a^2\,dt$. The effect of magnitude is essentially the same for all correlations with b equal to about 1. The coefficient c, which governs the rate of decay with distance is larger for accelerations and smaller for displacements, in agreement with what one would expect, since $\int_0^T a^2\,dt$ contains predominantly high-frequency waves which attenuate with distance more than the longer waves representing ground velocity and displacement. The standard deviation, σ, equal to about 0.5, is better than for correlations with the Modified Mercalli intensity (Table 2).

To examine the quality of the correlation (15) with distance, Δ, we assumed that the standard deviation may change with distance and computed coefficients A and B in the following linear equation

$$\sigma = A+B\log_{10}\Delta\pm\Sigma, \tag{16}$$

again using a least-squares fit. Those coefficients, and the standard deviation Σ, are also presented in Table 4. As can be seen from this table, the scatter of data is largest close to an earthquake source with the quality of fit improving for greater Δ. Consistently larger A and B for vertical components of ground motion indicate larger scatter in $\int_0^T a^2\,dt$, $\int_0^T v^2\,dt$, and $\int_0^T d^2\,dt$ for vertical components of ground motion and close to the source, but then a better fit as Δ increases.

Correlations of the Duration of Acceleration, Velocity and Displacement with the Modified Mercalli Intensity and Different Site Classifications

As already pointed out, we shall define the duration of strong-motion acceleration, velocity, and displacement to coincide with the interval of time during which the "significant" contributions to the integrals $\int_0^T a^2\,dt$, $\int_0^T v^2\,dt$, and $\int_0^T d^2\,dt$ take place. For definiteness, but otherwise quite arbitrarily, we select 90 per cent of the final amplitude, spaced between the 5 per cent and 95 per cent levels, to be that significant contribution. This procedure is illustrated in Figure 1 where an example of selecting the durations of acceleration, velocity, and displacement has been presented.

The above definition of duration is different from definitions used by some previous workers (Housner, 1965, 1970; Bolt, 1973). It is essentially based on that part of the recorded strong ground motion that generates 90 per cent of the overall acceleration, velocity, and displacement spectral amplitudes. Since the typical strong ground motion is represented by a dispersed train of waves, this definition automatically represents an upper bound for duration at any selected frequency or a frequency band.

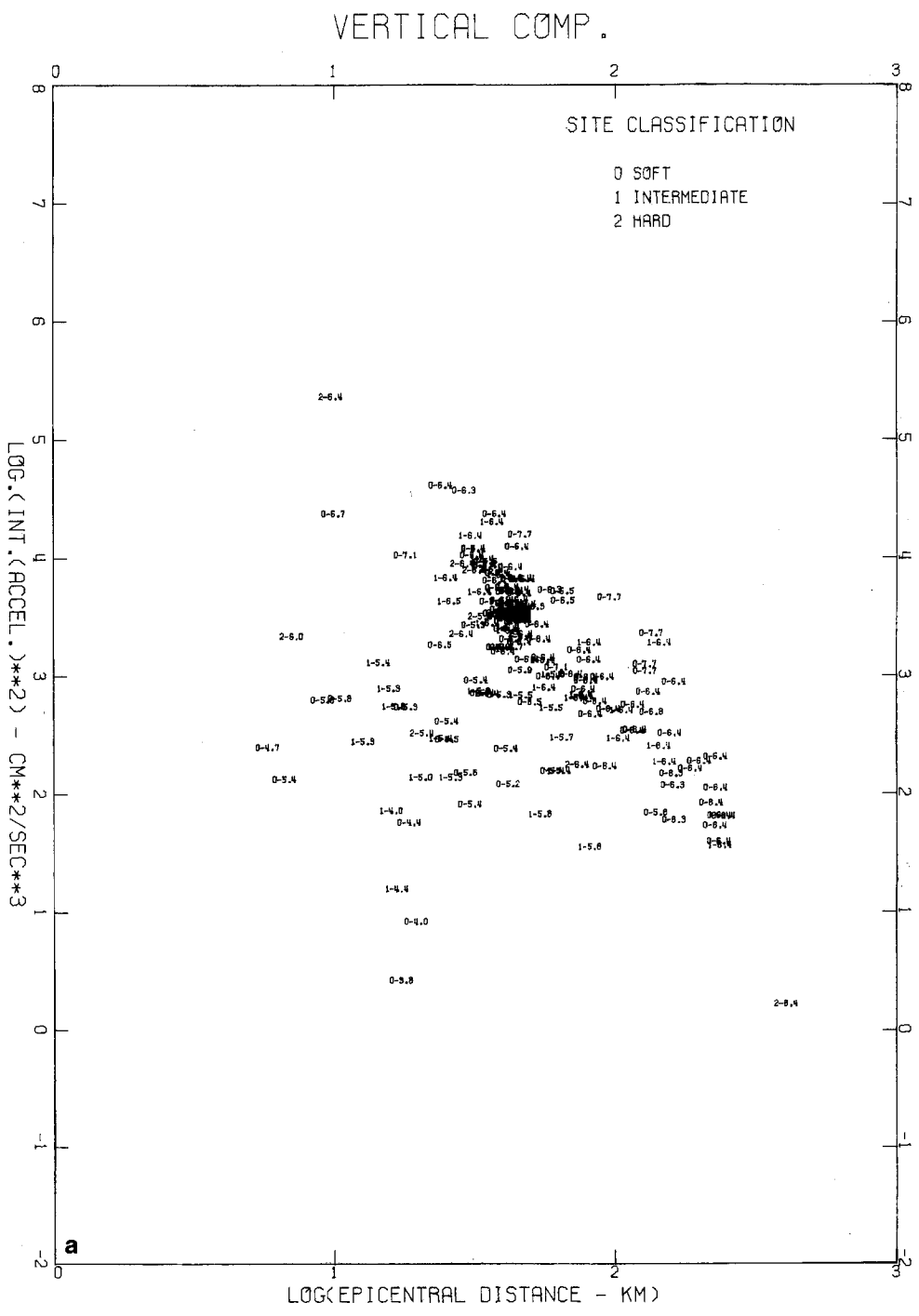

FIG. 4a. Correlation of the integral $\int_0^T a^2 dt$ for vertical components with site classification, magnitude, and epicentral distance.

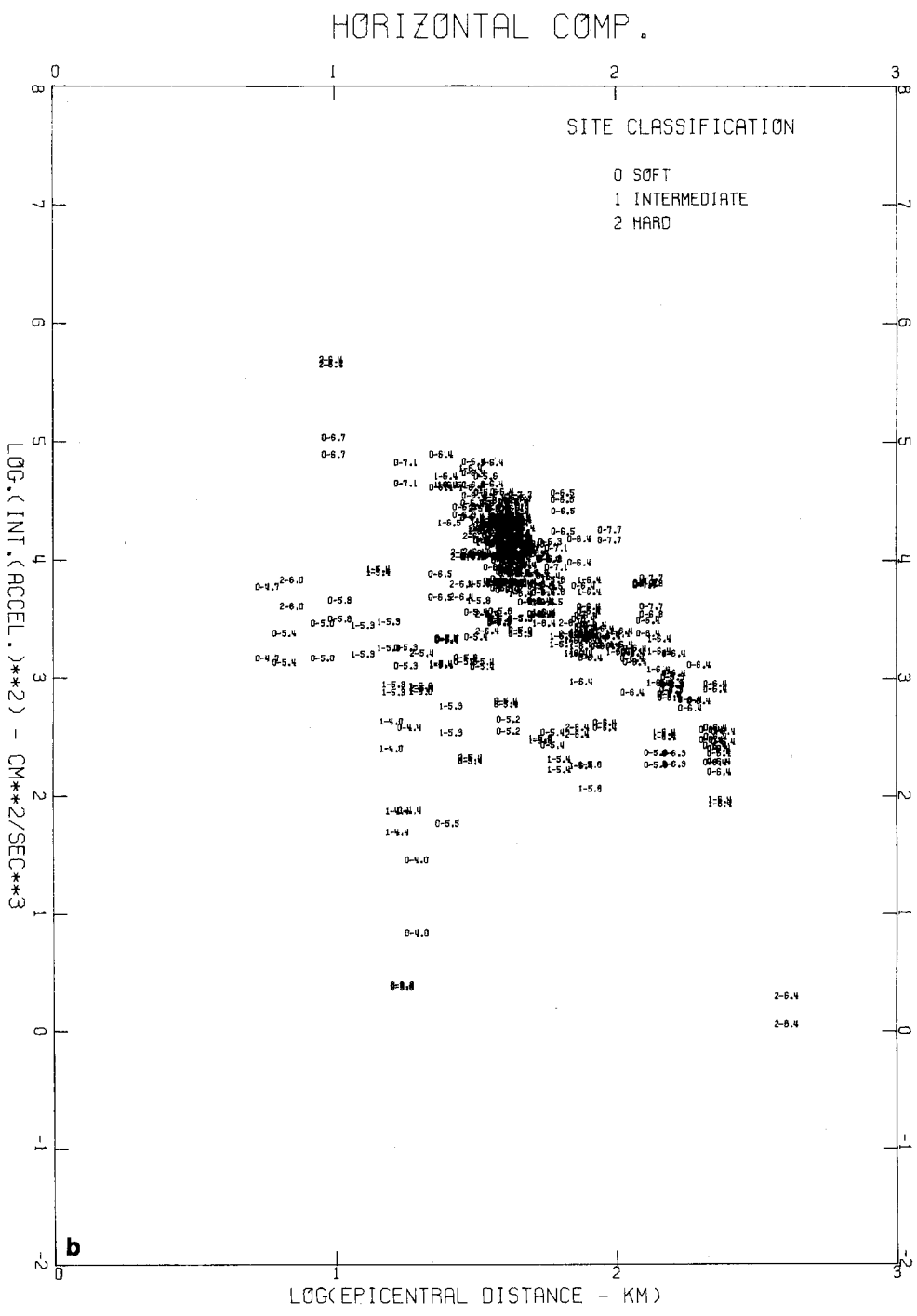

FIG. 4b. Correlation of the integral $\int_0^T a^2\,dt$ for horizontal components with site classification, magnitude, and epicentral distance.

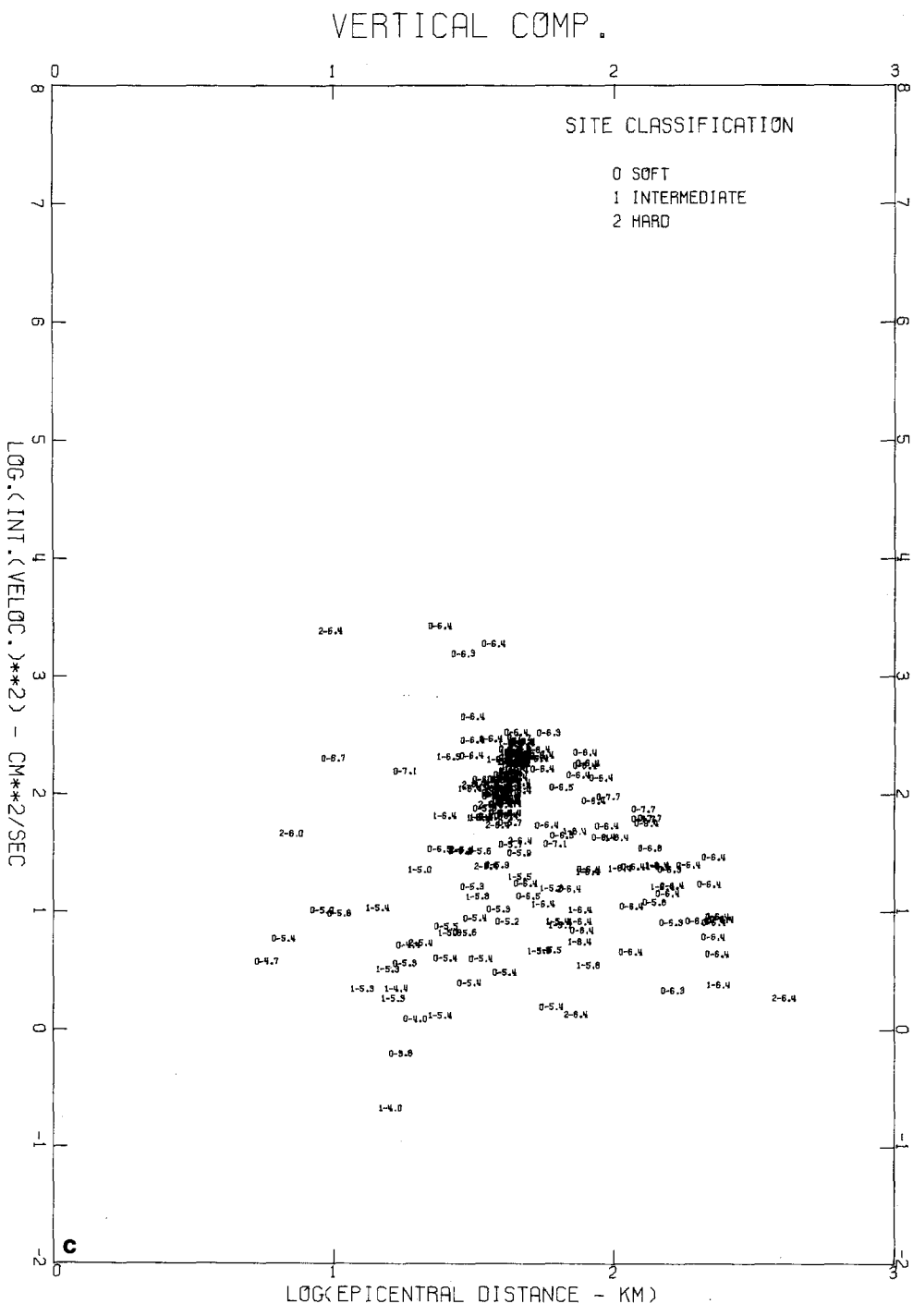

FIG. 4c. Correlation of the integral $\int_0^T v^2 dt$ for vertical components with site classification, magnitude, and epicentral distance.

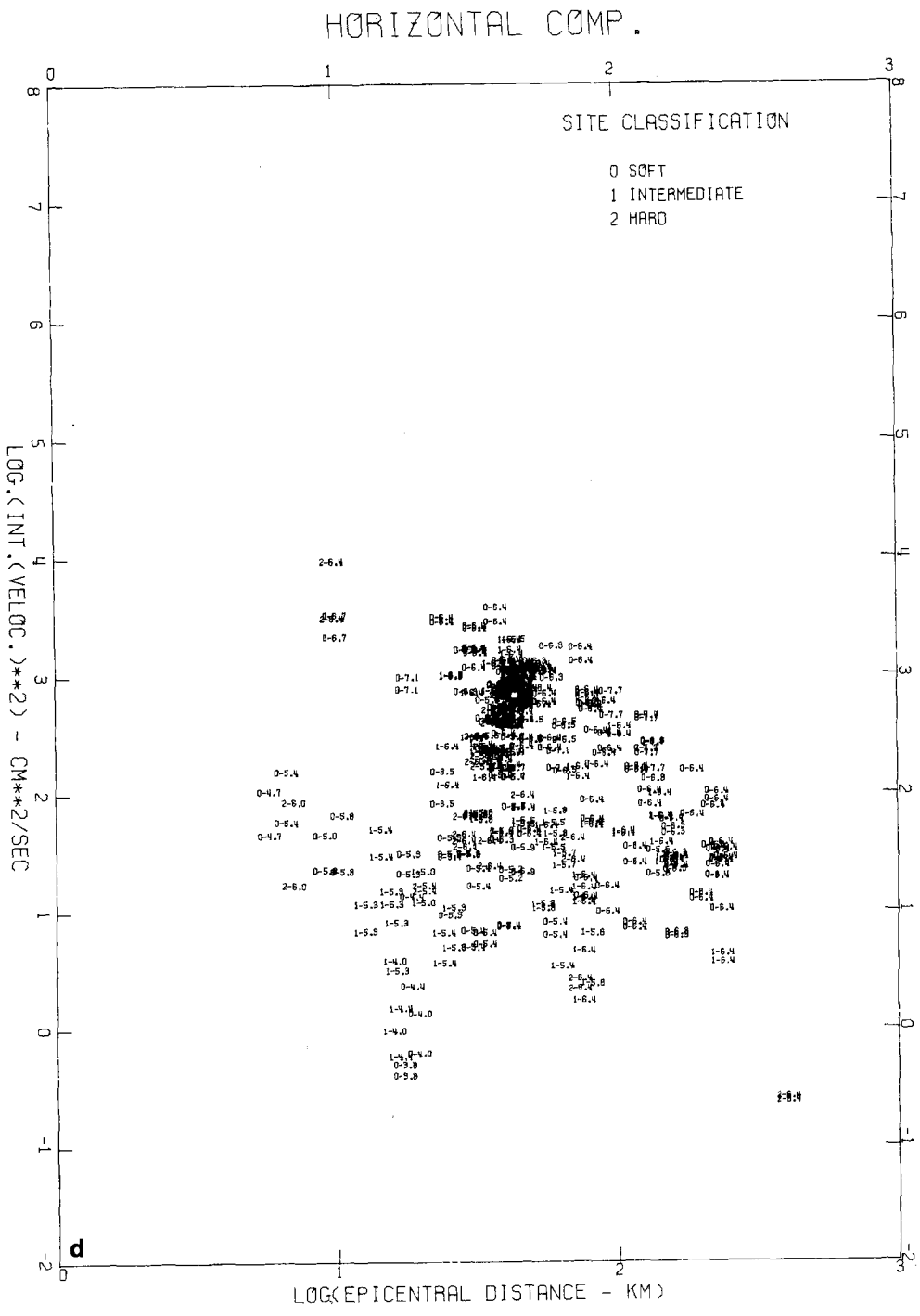

FIG. 4d. Correlation of the integral $\int_0^T v^2\,dt$ for horizontal components with site classification, magnitude, and epicentral distance.

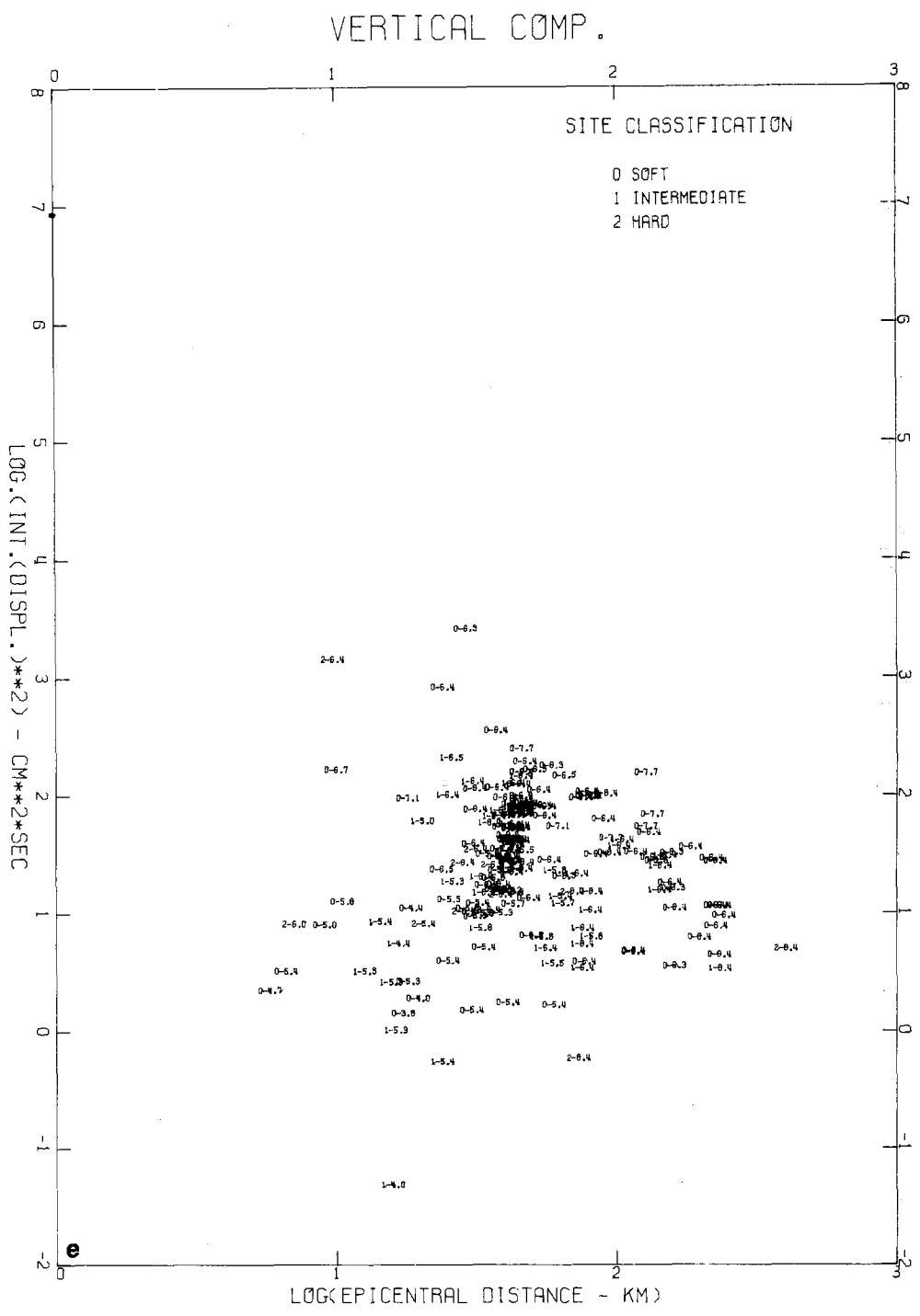

FIG. 4e. Correlation of the integral $\int_0^T d^2 dt$ for vertical components with site classification, magnitude, and epicentral distance.

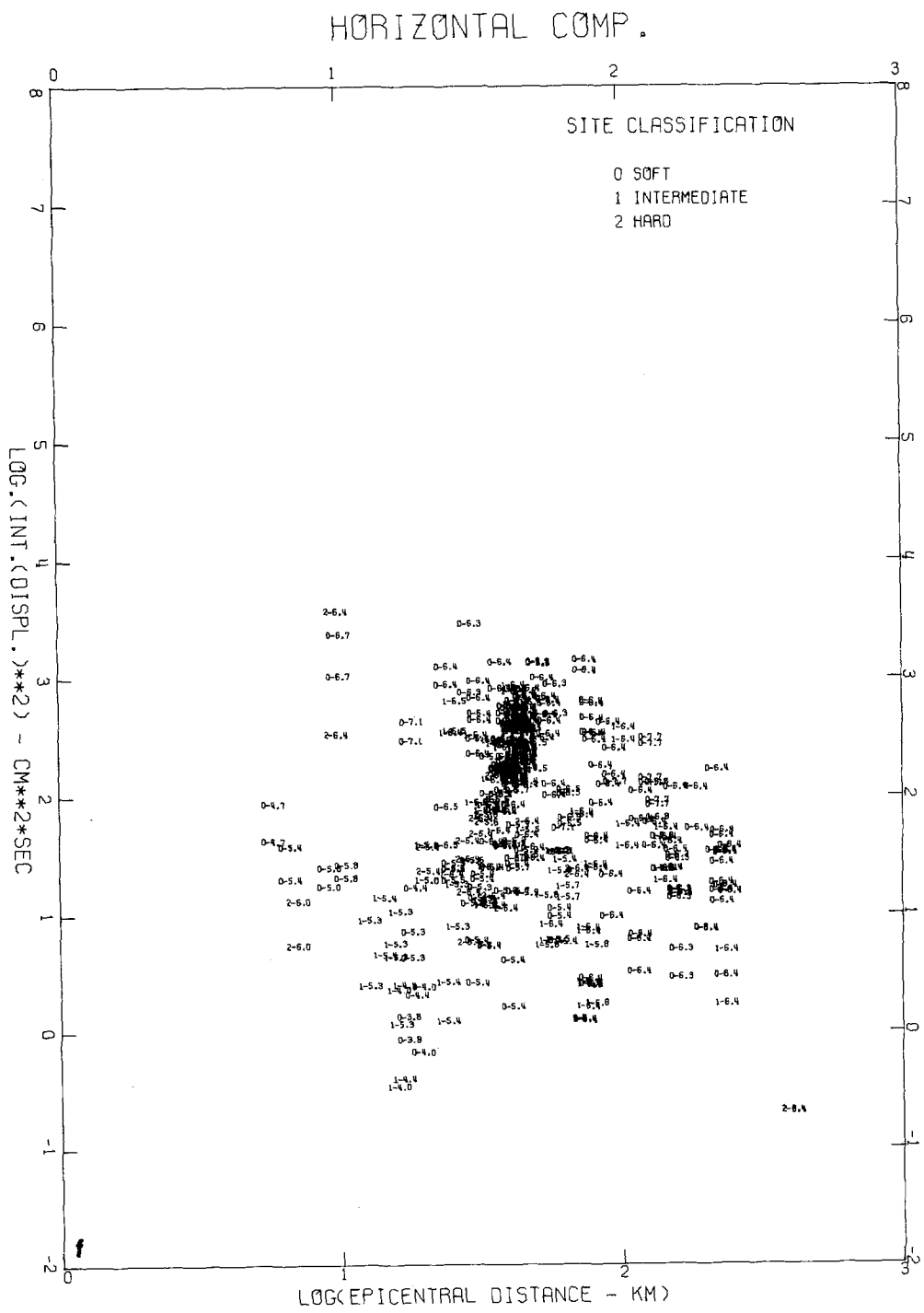

FIG. 4f. Correlation of the integral $\int_0^T d^2\,dt$ for horizontal components with site classification, magnitude, and epicentral distance.

TABLE 4

COEFFICIENTS IN EQUATIONS

$$\log_{10}\left\{\int_0^T \left(\begin{matrix}a^2\\v^2\\d^2\end{matrix}\right) dt\right\} = as+bM+c\log_{10}\Delta+d\pm\sigma;\quad \sigma = A+B\log_{10}\Delta\pm\Sigma.*$$

Component	a	b	c	d	σ	A	B	Σ	No. of Data
				Acceleration					
Vertical	−0.068	1.090	−1.79	−0.66	0.458	0.681	−0.200	0.290	181
Horizontal	−0.103	1.120	−1.87	−0.14	0.480	0.613	−0.156	0.321	362
				Velocity					
Vertical	−0.184	0.998	−1.10	−2.66	0.490	0.657	−0.158	0.286	181
Horizontal	−0.331	1.170	−1.44	−2.60	0.553	0.556	−0.061	0.316	362
				Displacement					
Vertical	−0.177	0.739	−0.62	−2.05	0.478	0.663	−0.172	0.288	181
Horizontal	−0.357	0.975	−1.14	−2.16	0.584	0.511	−0.020	0.336	362

*For site classifications s = 0, 1, and 2; earthquake magnitude, M; and epicentral distance, Δ.

Many strong-motion accelerograms taken from the Volume II series of corrected data (Hudson, *et al.*, 1971) have been digitized well past the strong-motion part resulting from the main earthquake event and frequently include one or more aftershocks. Since these aftershocks occasionally contribute a significant amount to the computed $\int_0^T a^2\,dt$, $\int_0^T v^2\,dt$, and $\int_0^T d^2\,dt$, the record lengths chosen for analysis have been selected in such a way as to eliminate these aftershocks and make computations of duration from the above integrals correspond to the duration of the main event only. For all records that have been analyzed using a reduced record length, the number in the brackets following the record identification number in Table 1 indicates the record length used in this paper. For all other records the original complete record length appearing in the Volume II series has been used in this analysis.

Figure 5 (a, b, and c) and Table 5 present the mean values and the corresponding standard deviations for the duration of acceleration, velocity, and displacement versus

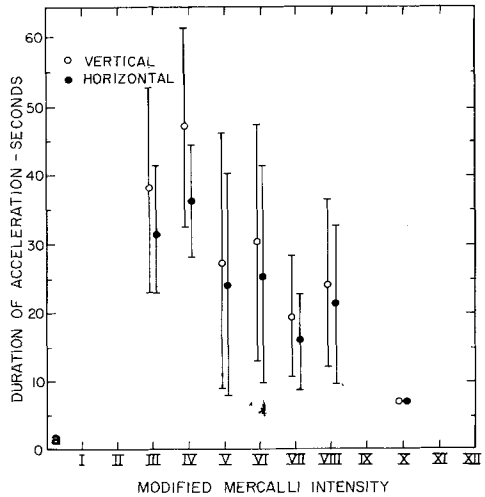

FIG. 5a. Calculated mean values and standard deviations of duration of acceleration, for vertical and horizontal components, at different Modified Mercalli intensities.

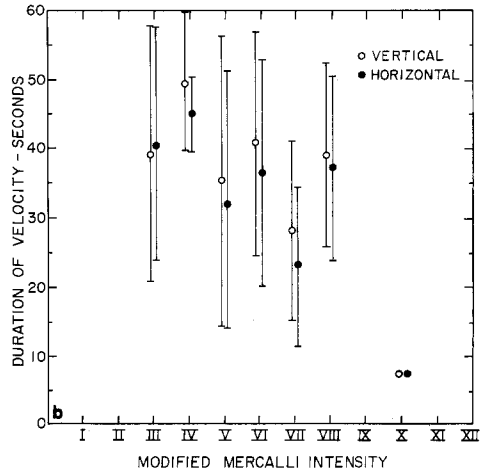

FIG. 5b. Calculated mean values and standard deviations of duration of velocity, for vertical and horizontal components, at different Modified Mercalli intensities.

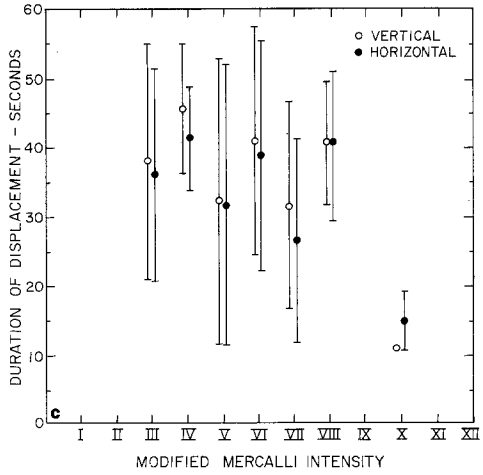

FIG. 5c. Calculated mean values and standard deviations of duration of displacement, for vertical and horizontal components, at different Modified Mercalli intensities.

Modified Mercalli intensity, as well as the number of the data points used in this analysis. The indicated trend is for the duration to decrease with increasing intensity level. This decrease is most pronounced for the duration of acceleration (Figure 5a) and least pronounced for the duration of ground displacement (Figure 5c) and can be explained by the dispersive nature of ground motion combined with the more pronounced attenuation of high-frequency waves with distance.

The duration value for intensity X has been derived from one accelerograph record only (Pacoima Dam accelerogram, C041) and thus may not be representative. It agrees with the extrapolated trend from the lower intensity data for the duration of acceleration, but it is shorter than the extrapolated durations of velocity and displacement data (Figure 5 (b and c). This may result from the fact that the San Fernando earthquake, although causing large strong-motion amplitudes, was in fact only a moderate magnitude earthquake fracturing only along a short fault, some 15 km long, and thus did not provide a representative average duration for the Modified Mercalli intensity level X.

The average duration of vertical ground motion is longer than the average duration of horizontal motion by several to about 10 sec. Although very small compared to one

TABLE 5

CORRELATION OF DURATION OF STRONG GROUND MOTION AND MODIFIED MERCALLI INTENSITY

Intensity	Component	Duration of Acceleration (sec)		Duration of Velocity (sec)		Duration of Displacement (sec)		No. of Data
		Mean	Standard deviation	Mean	Standard deviation	Mean	Standard deviation	
III	Vertical	38.0	15.0	39.0	18.0	38.0	17.00	2
	Horizontal	31.5	8.65	40.50	16.76	36.0	15.07	4
IV	Vertical	47.00	14.24	49.67	9.98	45.67	9.29	3
	Horizontal	36.33	8.06	45.00	5.16	41.33	7.34	6
V	Vertical	27.24	18.51	35.35	20.94	32.47	20.64	34
	Horizontal	24.03	16.05	32.62	18.77	31.88	20.09	68
VI	Vertical	30.39	17.19	40.76	15.99	40.64	16.24	66
	Horizontal	25.62	15.75	36.65	16.50	38.82	16.60	132
VII	Vertical	19.74	8.35	28.03	12.99	31.79	14.71	76
	Horizontal	15.87	7.03	23.01	11.54	26.62	14.87	151*
VIII	Vertical	24.33	12.04	39.00	13.42	40.67	8.83	6
	Horizontal	21.33	11.48	37.17	13.33	40.67	11.40	12
X	Vertical	7.00	—	7.00	—	11.00	—	1
	Horizontal	7.00	—	7.00	—	15.00	4.00	2

*See footnote of Table 2.

standard deviation of all data on duration, this difference is consistent for essentially all intensity levels presented in Figure 5 (a, b, and c). We are not aware of any simple physical reasons for such differences, but suspect that the causes may be associated with the predominantly horizontal stratification of alluvial deposits.

The approximate trends of the mean duration of acceleration, velocity, and displacement versus Modified Mercalli intensity, I_{MM}, may be described by the following equations

$$\text{Duration of acceleration} = \begin{cases} 56.3 - 4.67\, I_{MM} \text{ for vertical components} \\ 46.5 - 3.85\, I_{MM} \text{ for horizontal components} \end{cases} \tag{17}$$

$$\text{Duration of velocity} = \begin{cases} 55.5 - 2.75\, I_{MM} \text{ for vertical components} \\ 58.4 - 3.75\, I_{MM} \text{ for horizontal components} \end{cases} \tag{18}$$

$$\text{Duration of displacement} = \begin{cases} 45.2 - 0.827\, I_{MM} \text{ for vertical components} \\ 41.8 - 0.674\, I_{MM} \text{ for horizontal components} \end{cases} \tag{19}$$

and for $\text{III} \leqq I_{MM} \leqq \text{VIII}$.

These trends are characterized by one standard deviation which is less than about 20 sec.

To study the effects the geological environment might have on the duration of strong earthquake ground motion and for different Modified Mercalli intensities, the above data on duration was divided into three groups corresponding to the records obtained on "soft" (0), "intermediate" (1), and "hard" basement rocks (2). Table 6 summarizes the results of such division of data and gives the number of data used for various intensity

TABLE 6

DURATION OF STRONG GROUND MOTION FOR DIFFERENT MODIFIED MERCALLI INTENSITIES AND SITE CONDITIONS (0, 1 AND 2)

Intensity	Composition	Duration of Acceleration		Duration of Velocity		Duration of Displacement		No. of Data
		Mean	Standard deviation	Mean	Standard deviation	Mean	Standard deviation	
III–0	Vertical	53.0	—	57.00	—	55.00	—	1
	Horizontal	39.00	6.00	57.00	4.00	51.00	2.00	2
III–1	Vertical							
	Horizontal							
III–2	Vertical	23.0	—	21.00	—	21.00	—	1
	Horizontal	24.0	1.00	24.00	1.00	21.00	—	2
IV–0	Vertical	67.0	—	63.00	—	55.00	—	1
	Horizontal	46.00	3.00	50.00	5.00	51.00	2.00	2
IV–1	Vertical	37.00	2.00	43.00	4.00	41.00	8.00	2
	Horizontal	31.50	4.77	42.50	2.96	36.50	2.96	4
IV–2	Vertical							
	Horizontal							
V–0	Vertical	33.59	20.62	42.76	22.05	40.65	22.66	17
	Horizontal	28.12	17.17	39.18	19.53	39.18	21.15	34
V–1	Vertical	21.93	13.83	29.00	17.19	25.27	14.68	15
	Horizontal	21.00	14.19	27.33	15.57	25.87	16.22	30
V-2	Vertical	13.00	4.00	20.00	9.00	17.00	8.00	2
	Horizontal	12.00	3.00	16.50	9.53	15.00	9.06	4
VI–0	Vertical	35.88	17.24	42.49	14.73	41.84	15.68	43
	Horizontal	30.53	15.96	38.60	16.02	39.84	15.82	86
VI–1	Vertical	23.75	11.72	43.50	17.66	42.38	17.08	16
	Horizontal	18.75	11.26	36.81	17.32	40.81	18.15	32
VI–2	Vertical	11.86	4.12	23.86	6.75	29.29	12.85	7
	Horizontal	11.14	4.37	23.43	10.37	28.00	13.22	14
VII–0	Vertical	22.48	8.13	32.28	12.83	35.56	13.87	50
	Horizontal	18.54	6.58	26.94	11.58	29.91	15.34	99*
VII–1	Vertical	15.76	5.64	21.38	8.30	25.86	14.51	21
	Horizontal	12.14	3.83	16.10	6.93	20.95	12.34	42
VII–2	Vertical	9.00	3.10	13.40	6.97	19.00	5.37	5
	Horizontal	5.20	3.52	13.20	5.76	17.80	7.17	10
VIII–0	Vertical	24.33	12.04	39.00	13.42	40.67	8.83	6
	Horizontal	21.33	11.48	37.17	13.33	40.67	11.40	12
VIII–1	Vertical							
	Horizontal							
VIII–2	Vertical							
	Horizontal							
X–0	Vertical							
	Horizontal							
X–1	Vertical							
	Horizontal							
X–2	Vertical	7.00	—	7.00	—	11.00	—	1
	Horizontal	7.00	—	7.00	—	15.00	4.00	2

*See footnote of Table 2.

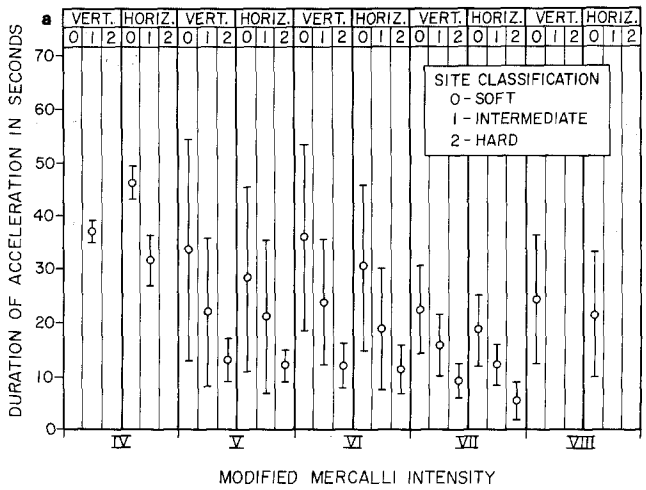

FIG. 6a. Calculated mean values and standard deviations of duration of acceleration, for vertical and horizontal components, at different site classifications and Modified Mercalli intensities.

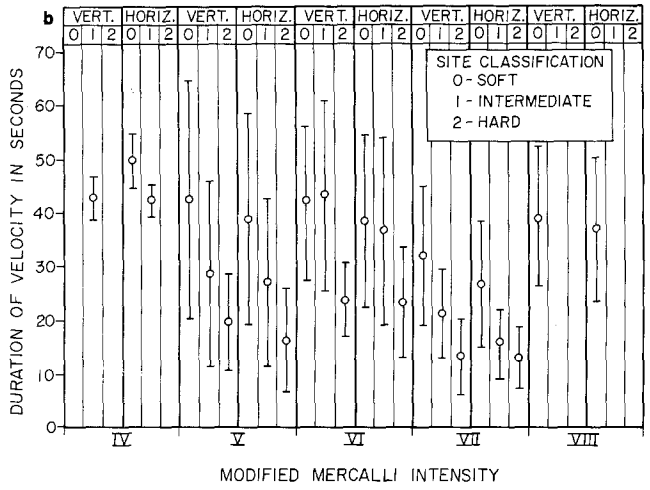

FIG. 6b. Calculated mean values and standard deviations of duration of velocity, for vertical and horizontal components, at different site classifications and Modified Mercalli intensities.

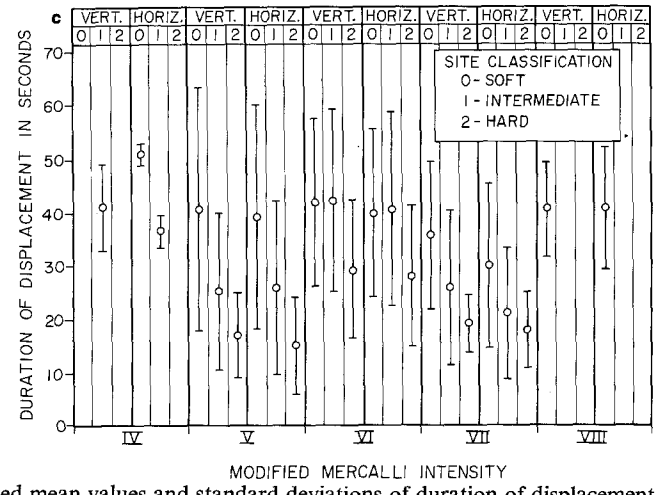

FIG. 6c. Calculated mean values and standard deviations of duration of displacement, for vertical and horizontal components, at different site classifications and Modified Mercalli intensities.

levels and site classifications. Figure 6 (a, b, and c) where the means and the corresponding standard deviations for different Modified Mercalli intensities have been plotted shows the same correlations.

The effect of geological environment of a recording site seems to be clear and consistent for Modified Mercalli intensities V, VI ,and VII for which the present data-set seems to be adequate. The average duration of strong ground motion is about twice as long on "soft" alluvium as on hard-base rock. This trend is essentially the same for ground acceleration, velocity, and displacement [Figure 6 (a, b, and c)]. Again, the duration of the vertical component of ground motion is on the average several seconds longer than the duration of the horizontal components.

Correlations of the Duration of Acceleration, Velocity, and Displacement with Magnitude, Epicentral Distance, and Local Site Classification

Figure 7 (a to f) shows all data on the duration of acceleration, velocity, and displacement plotted versus the logarithm of epicentral distance. The corresponding site classification and earthquake magnitude are also indicated. As can be seen from this figure, the scatter of data on duration is appreciable and no simple and obvious trend with distance or magnitude is apparent. To reduce this scatter, one may try to derive an empirical model that will reflect the average trends of data for different site conditions, earthquake magnitudes, and epicentral distances.

The first step in deriving an empirical model for the data in Figure 7 is to determine the functional form of the correlations between the duration and the respective parameters that describe the earthquake and the recording site. The least understood functional relationship of this type is that between the duration and the site classification. This is so because the precision with which one can classify a given site as being 0, 1, or 2 is not always good and the classification system we employ (Trifunac and Brady, 1975) is quite rough and neglects many other parameters which describe the recording site in greater detail. Furthermore, even if one were to classify the recording sites in a more precise and detailed manner, the serious shortage of theoretical work relating such site classification with the duration of scattered and diffracted wave forms would, at this time, render more detailed site description useless.

We propose to analyze the duration of strong ground motion as a sum

$$\text{duration of} \begin{Bmatrix} \text{acceleration} \\ \text{velocity} \\ \text{displacement} \end{Bmatrix} = d_s + d_{\text{source}} + d_\Delta \tag{20}$$

where d_{source} represents the duration of the earthquake source, d_Δ is the time interval between the fastest and the slowest wave arrival at a station which is at Δ kilometers from the source, and d_s is the additional duration of shaking caused by repeated wave scattering from different material discontinuities and from surface topography. We expect that it is this d_s that will reflect the influence of site classification.

The duration of an earthquake source seems to be most directly related to the fault length. Although not all earthquakes can be characterized by a fault rupture initiated at one end and by a dislocation propagating toward the other end of the fault, the first approximation to the duration of an earthquake source would be the fault length divided by the average dislocation velocity. Using the average trend of data presented by Thatcher and Hanks (1973) an approximate correlation of earthquake magnitude, M, and the fault

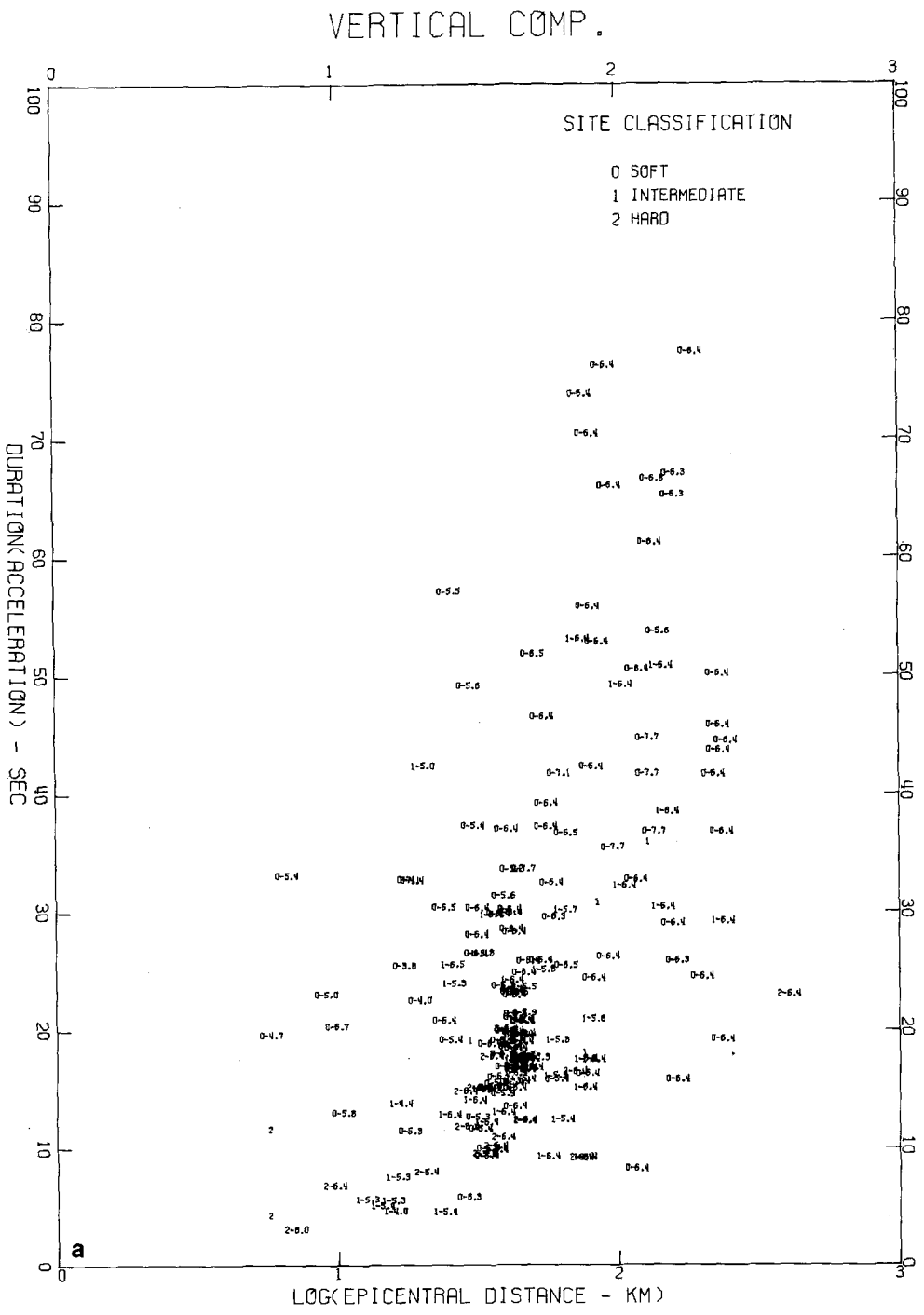

FIG. 7a. Correlation of the duration of the vertical component of acceleration with site classification, magnitude, and epicentral distance.

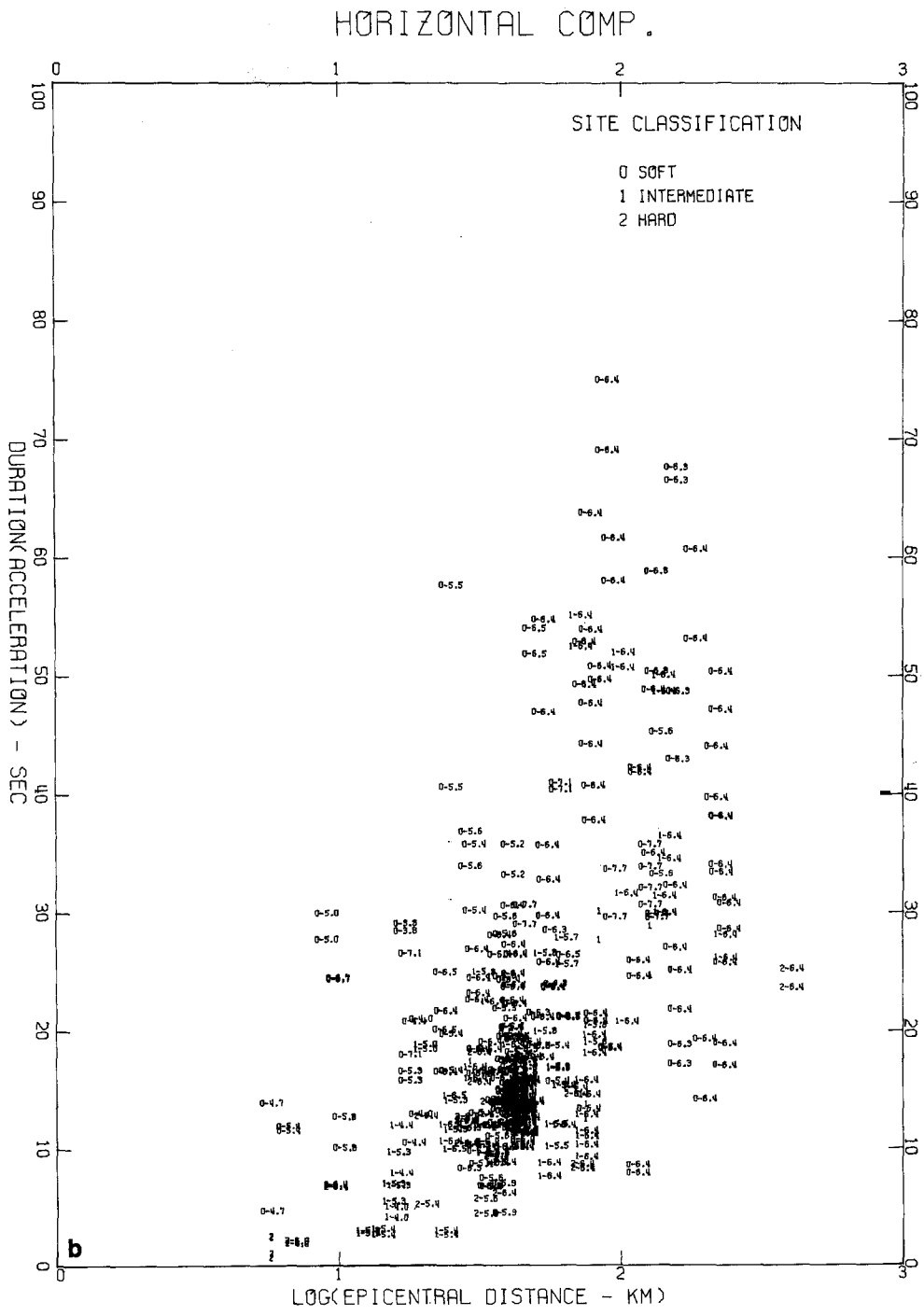

FIG. 7b. Correlation of the duration of the horizontal component of acceleration with site classification, magnitude, and epicentral distance.

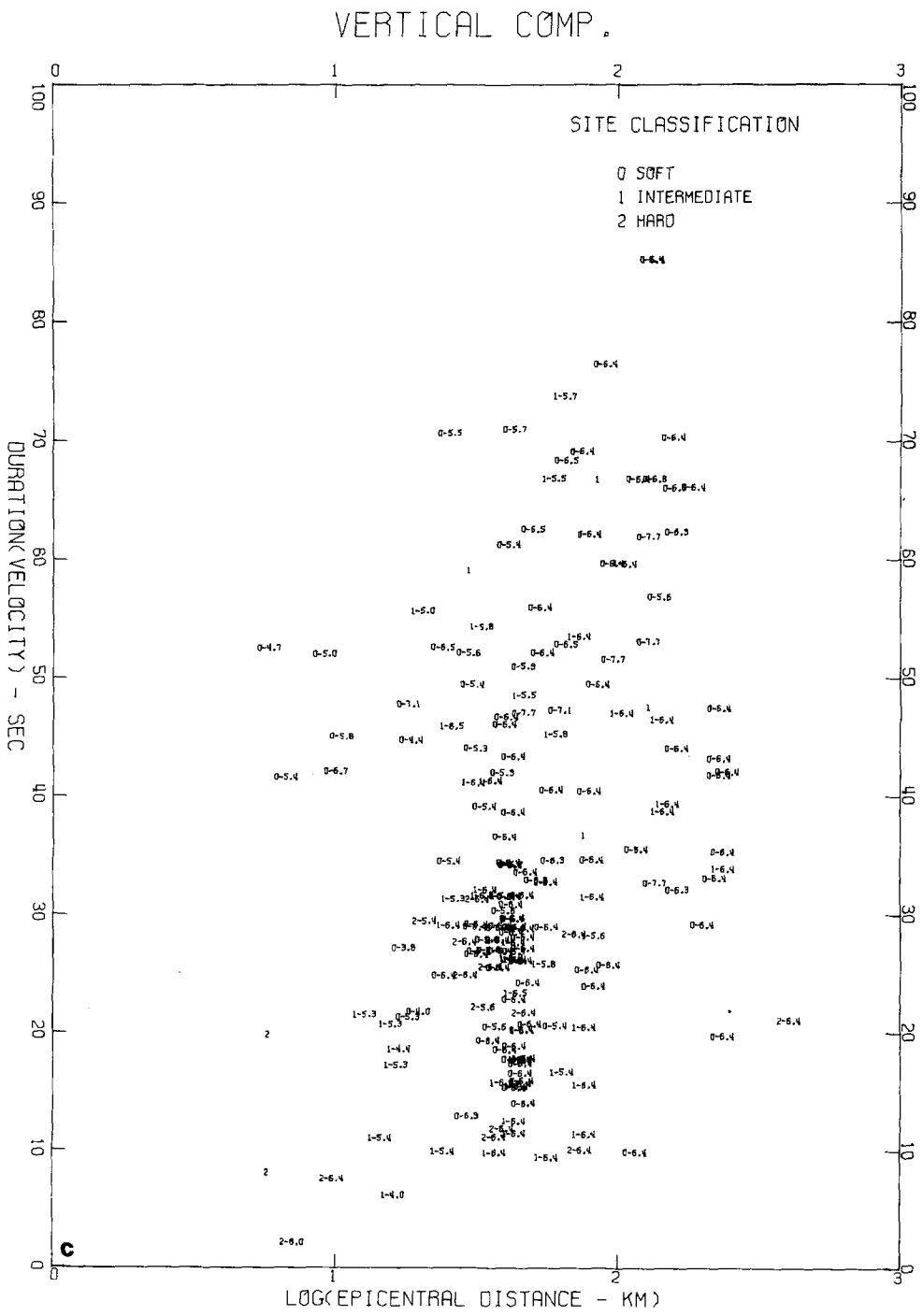

FIG. 7c. Correlation of the duration of the vertical component of velocity with site classification, magnitude, and epicentral distance.

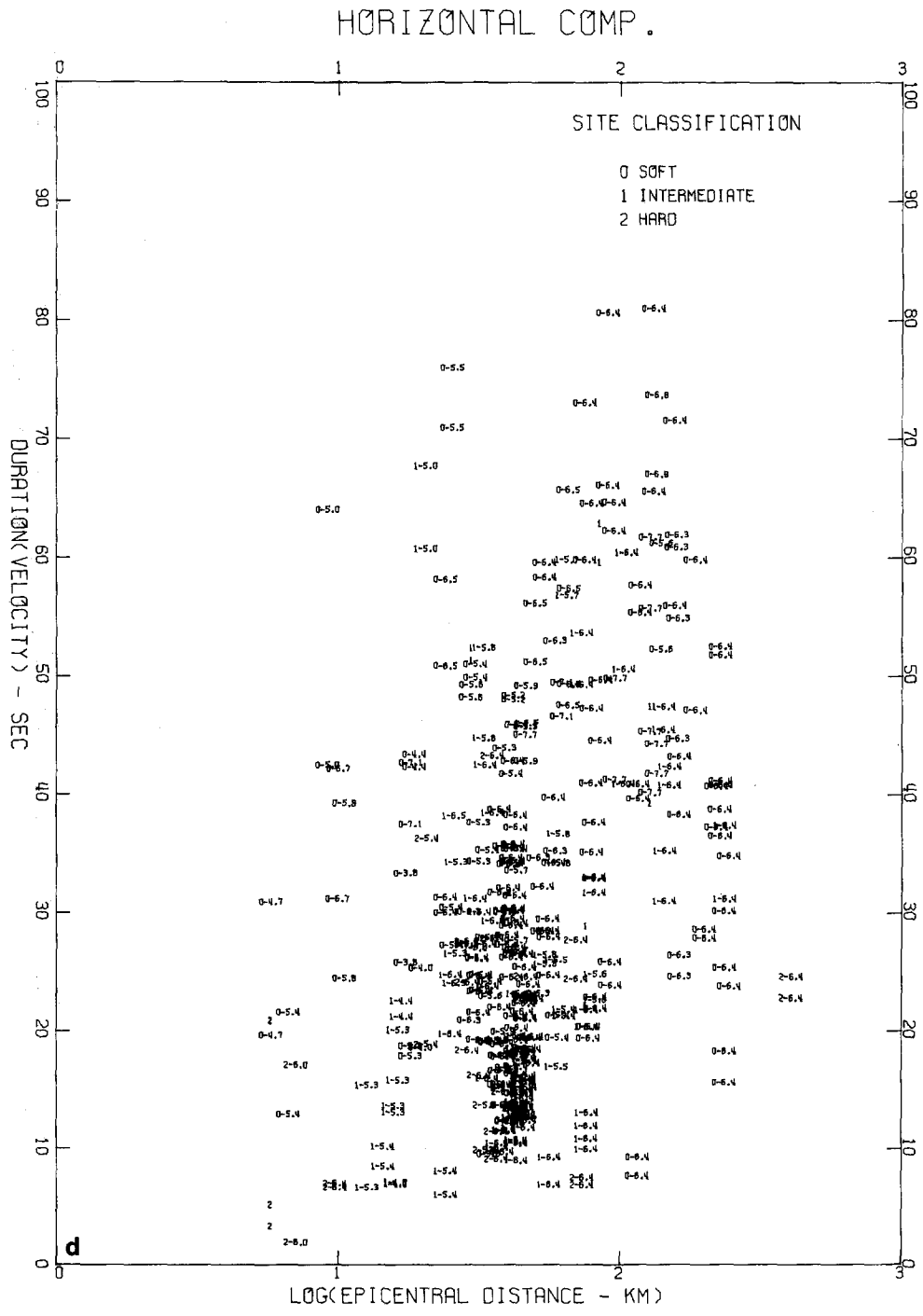

FIG. 7d. Correlation of the duration of the horizontal component of velocity with site classification, magnitude, and epicentral distance.

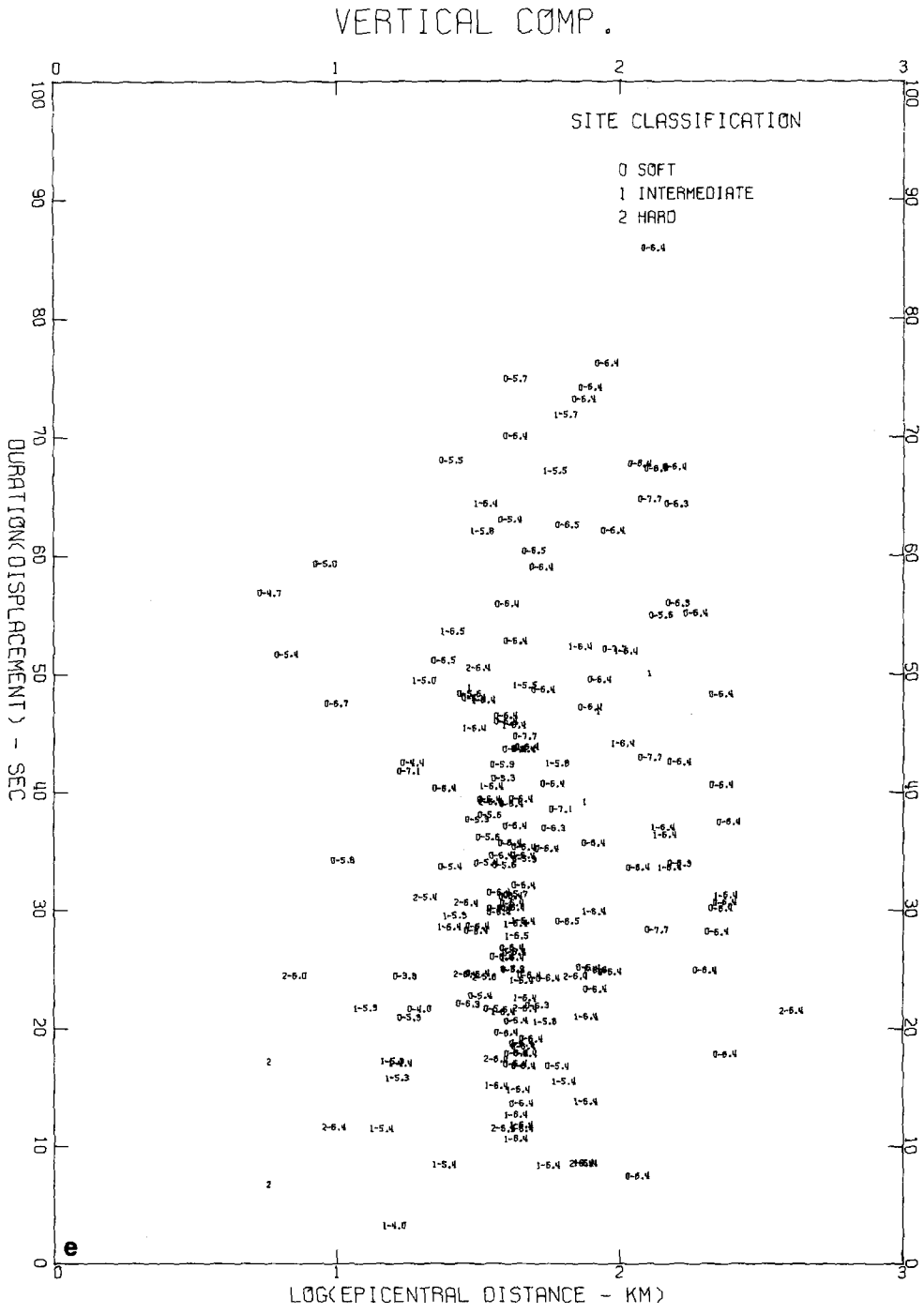

FIG. 7e. Correlation of the duration of the vertical component of displacement with site classification, magnitude, and epicentral distance.

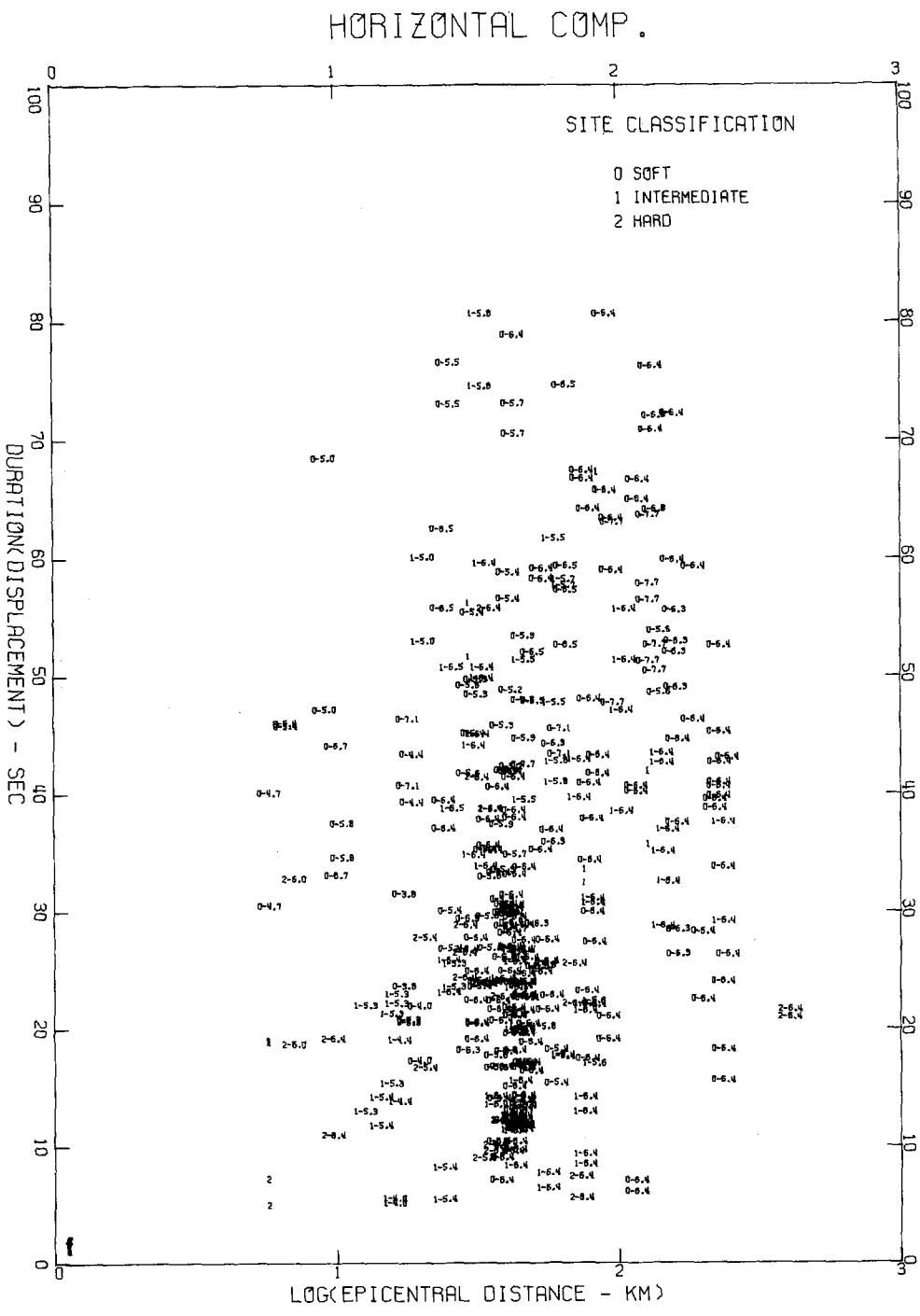

FIG. 7f. Correlation of the duration of the horizontal component of displacement with site classification, magnitude, and epicentral distance.

length, L, in kilometers would be

$$M \approx 3+2 \log_{10} L. \tag{21}$$

For a dislocation velocity of about 3 km/sec this would give the source duration, d_{source}, in seconds as

$$d_{\text{source}} \approx 10^{(M/2)-2}. \tag{22}$$

It must be remembered, however, that for many earthquakes the faulting may not progress uniformly along the fault, but is often represented by a sequence of multiple events (e.g., Wyss and Brune, 1967; Trifunac, 1972; Trifunac, 1974) which can lead to large variations of the source duration. Furthermore, since the data used in this paper result from a narrow range of assigned magnitudes (almost all data fall in the magnitude range 4 to 6.5), we shall simplify the expression for the source duration to

$$d_{\text{source}} = bM, \tag{23}$$

where b is a constant. This simplification has another advantage in that it leads to linear regression analysis and an easy evaluation of the constant b.

The contribution to the total duration that results from dispersion and from the fact that different waves propagate with different velocities, d_Δ, is clearly a linear function of the source-to-station distance. To simplify the analysis and because the source-to-station distance cannot be computed for all accelerograph records since hypocentral depth and the orientation of the fault plane are not known for most of the 57 earthquakes (see Table 2 of Trifunac and Brady, 1975) studied in this paper, we will use the epicentral distance, Δ, instead, so that

$$d_\Delta = c\Delta. \tag{24}$$

The constant c could be calculated from

$$c = \frac{1}{V_{\min}} - \frac{1}{V_{\max}}, \tag{25}$$

where $V_{\max}$ and $V_{\min}$ represent the velocities of the fastest and the slowest waves in a given region. Taking, for example, $V_{\max} = 6$ km/sec and $V_{\min} = 3$ km/sec, one gets $c = 0.16$. However, since the strong-motion acceleration, velocity and displacement display predominantly different frequency bands and thus emphasize different wave types, we shall compute c from linear regression analysis rather than from equation (25).

Rewriting equation (20) in terms of the above proposed approximations for d_s, d_{source}, and d_Δ, we have the approximate model

$$\text{duration of} \begin{Bmatrix} \text{acceleration} \\ \text{velocity} \\ \text{displacement} \end{Bmatrix} = as+bM+c\Delta \pm \sigma, \tag{26}$$

where a is the site-dependent constant, s takes on discrete values of 0, 1, or 2, and σ is one standard deviation. Table 7 presents the regression coefficients for this model and the number of data points used. As seen from this table, 106 rather than 188 accelerograms have been used in this regression. This reduction results from the requirement we imposed on the selection of accelerograms which has been that the total duration of a record must be more than 20 per cent longer than the duration of strong ground motion computed from the 90 per cent amplitudes as $\int_0^T a^2\,dt$, $\int_0^T v^2\,dt$, and $\int_0^T d^2\,dt$ (Figure 1). This requirement was imposed to eliminate a possible sensitivity of the regression coefficients on too early termination of a digitized record.

The coefficients in Table 7 show that an average strong ground motion lasts 8 to 12 sec longer at a "soft" site than on a "hard" site. The magnitude dependence is largest for the duration of the displacement and then decreases for velocity and acceleration. Coefficient c is largest for acceleration indicating more important influence of dispersion and larger separation of V_{max} and V_{min} for the higher frequency part of strong motion. The standard deviation of the estimated duration is about 10 sec for the duration of strong-motion acceleration and about 14 sec for the duration of strong-motion displacement.

TABLE 7

COEFFICIENTS IN THE EQUATIONS

$$\text{Duration}\begin{Bmatrix}\text{acceleration}\\ \text{velocity}\\ \text{displacement}\end{Bmatrix} = as+bM+c\Delta\pm\sigma; \quad \sigma(\text{duration}) = A+B\Delta\pm\Sigma.*$$

Component	a	b	c	σ	A	B	Σ	No. of Data
				Acceleration				
Vertical	−6.29	2.90	0.172	10.89	4.21	0.0672	7.25	106
Horizontal	−4.88	2.33	0.149	10.67	2.92	0.0830	7.17	212
				Velocity				
Vertical	−6.51	4.50	0.100	12.13	8.53	0.0221	7.25	106
Horizontal	−5.60	3.55	0.141	12.16	6.94	0.0519	7.14	212
				Displacement				
Vertical	−5.82	5.32	0.0307	13.61	10.19	0.00397	8.78	106
Horizontal	−4.08	4.07	0.107	13.72	10.10	0.0152	8.31	212

*For site classifications s = 0, 1, and 2, earthquake magnitude, M, and epicentral distance, Δ.

If one assumes that a significant contribution to the standard deviations in Table 7 is caused by inhomogeneous media through which seismic waves propagate, then it would be reasonable to suppose that the standard deviation of the estimated duration would increase with distance, since the number and the complexity of scattering obstacles grows with distance. If one assumes that such trends might be approximated by

$$\sigma(\text{duration}) = A+B\Delta\pm\Sigma, \tag{27}$$

then the coefficients A and B in Table 7 suggest that the standard deviation indeed grows with distance. This growth is appreciable for the duration of acceleration and slight for the duration of displacement. This means that the high-frequency acceleration waves must encounter more obstacles along the same traveled distance, Δ, than do the low-frequency displacement waves. Since the high-frequency waves are associated with short wavelengths and since those are also more sensitive to the inhomogeneities along the propagation path (Trifunac, 1971; Trifunac, 1973; Wong and Trifunac, 1974a; Wong and Trifunac, 1974b), the variation of the coefficients in Table 7 appears to be in accord with our physical intuition.

We studied other forms of equation (26) to see whether the standard deviations shown in Table 7 can be further reduced. In one of these trials we added a constant term, d, to equation (26) and in another we assumed that $d_\Delta = c \log_{10} \Delta$. These tests have indicated

that the equation (26) represents the best choice for a simple, first-order, approximation of the duration of the strong ground motion.

Correlations of the Rate of Growth of Strong Ground Motion with Modified Mercalli Intensity and Different Site Classifications

As we have already pointed out, the rate of growth of the integrals $\int_0^T a^2\,dt$, $\int_0^T v^2\,dt$, and $\int_0^T d^2\,dt$ as defined by equation (11) may be quite useful in response computations based on the energy balance and when non linear and deteriorating structural models have to be considered. Although this rate could be computed from the ratio of the established correlations between these integrals and the Modified Mercalli intensity and from the correlations of the duration of strong ground motion also with the Modified Mercalli intensity, to avoid cumulative effects of simple assumptions, we develop here these correlations directly.

Figure 8 (a, b and c) and Table 8 present the rate of vertical and horizontal strong-motion acceleration, velocity, and displacement versus Modified Mercalli intensity. The approximate trend of the logarithm of the rate of strong motion correlates linearly with the Modified Mercalli intensity, but the rates of velocity and displacement, especially for the vertical component, tend to level off for low intensities. This is caused by similar trends which were previously pointed out for Figure 2 (b and c), where the presence of low-frequency digitization noise (Trifunac, Udwadia, and Brady, 1973) in the records of small accelerations tends to increase the values of $\int_0^T v^2\,dt$ and $\int_0^T d^2\,dt$. When these low intensity levels are omitted, all average rates correlate with the Modified Mercalli intensity, I_{MM}, in an approximately linear manner as follows

$$\log_{10}\left[\left(\int_0^T a^2\,dt\right)/\text{duration}\right] = \left.\begin{cases} -1.99+0.597\,I_{MM} \text{ for vertical accelerations} \\ -1.17+0.560\,I_{MM} \text{ for horizontal accelerations} \end{cases}\right\} \quad (28)$$
$$\text{for III} \leqq I_{MM} \leqq \text{VIII}$$

$$\log_{10}\left[\left(\int_0^T v^2\,dt\right)/\text{duration}\right] = \left.\begin{cases} -2.61+0.420\,I_{MM} \text{ for vertical velocities} \\ -2.43+0.469\,I_{MM} \text{ for horizontal velocities} \end{cases}\right\} \quad 29)$$
$$\text{for V} \leqq I_{MM} \leqq \text{VIII}$$

and

$$\log_{10}\left[\left(\int_0^T d^2\,dt\right)/\text{duration}\right] = \left.\begin{cases} -2.10+0.315\,I_{MM} \text{ for vertical displacements} \\ -2.39+0.417\,I_{MM} \text{ for horizontal displacements} \end{cases}\right\} (30)$$
$$\text{for V} \leqq I_{MM} \leqq \text{VIII}$$

The effect of site conditions on the rate of acceleration, velocity, and displacement has been presented in Figure 9 (a, b, and c) and in Table 9. The available data indicate larger rates for strong-motion acceleration on "hard" basement rocks than on "soft" alluvium and for Modified Mercalli intensities V and VI. For intensity VII this trend is lost and no significant differences can be observed for different site classifications. The possible effect of site conditions on the rate of strong-motion displacement corresponding to Modified Mercalli intensities V and VI is overshadowed by the random fluctuations in the data. However, larger rates for "soft" sites for intensity VII may be indicated. The trends of the rate of strong-motion velocity seem to be half-way between those of acceleration and displacement indicated in Figure 9 (a and c) but if real are too small to be identified from the data in Figure 9b alone.

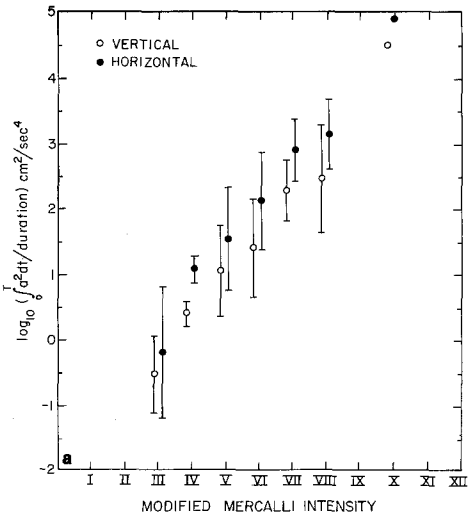

FIG. 8a. Mean values and standard deviations of the rate of growth of the integral $\int_0^T a^2\,dt$ for vertical and horizontal components and different Modified Mercalli intensities.

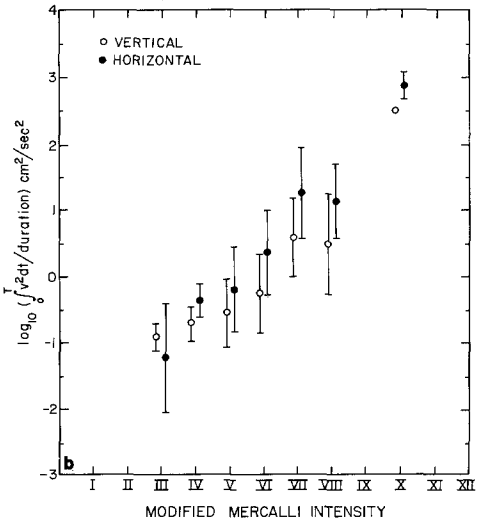

FIG. 8b. Mean values and standard deviations of the rate of growth of the integral $\int_0^T v^2\,dt$ for vertical and horizontal components and different Modified Mercalli intensities.

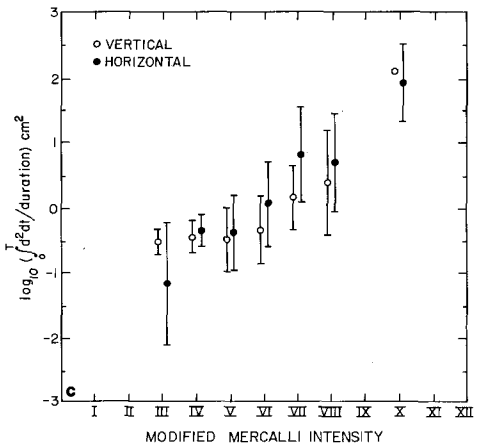

FIG. 8c. Mean values and standard deviations of the rate of growth of the integral $\int_0^T d^2\,dt$ for vertical and horizontal components and different Modified Mercalli intensities.

TABLE 8

CORRELATION OF THE RATE OF VERTICAL AND HORIZONTAL STRONG-MOTION ACCELERATION, VELOCITY AND DISPLACEMENT WITH MODIFIED MERCALLI INTENSITY

Intensity	Component	$\log_{10}[\int_0^T a^2 dt/\text{dur.}, (\text{cm}^2/\text{sec}^4)]$		$\log_{10}[\int_0^T v^2 dt/\text{dur.}, (\text{cm}^2/\text{sec}^2)]$		$\log_{10}[\int_0^T d^2 dt/\text{dur.}, (\text{cm}^2)]$		No. of Data
		Mean	Standard deviation	Mean	Standard deviation	Mean	Standard deviation	
III	Vertical	−0.50	0.60	−0.90	0.20	−0.50	0.20	2
	Horizontal	−0.20	1.00	−1.20	0.81	−1.15	0.95	4
IV	Vertical	0.43	0.19	−0.70	0.28	−0.43	0.25	3
	Horizontal	1.10	0.20	−0.37	0.25	−0.33	0.24	6
V	Vertical	1.07	0.71	−0.52	0.51	−0.48	0.49	34
	Horizontal	1.55	0.80	−0.20	0.65	−0.36	0.59	68
VI	Vertical	1.41	0.76	−0.21	0.61	−0.31	0.52	66
	Horizontal	2.12	0.76	0.38	0.66	0.10	0.67	132
VII	Vertical	2.29	0.46	0.62	0.61	0.17	0.50	76
	Horizontal	2.92	0.48	1.29	0.70	0.84	0.73	151*
VIII	Vertical	2.47	0.83	0.50	0.78	0.40	0.81	6
	Horizontal	3.12	0.53	1.13	0.58	0.73	0.77	12
X	Vertical	4.50	—	2.50	—	2.10	—	1
	Horizontal	4.90	—	2.90	0.20	1.90	0.60	2

*See footnote to Table 2.

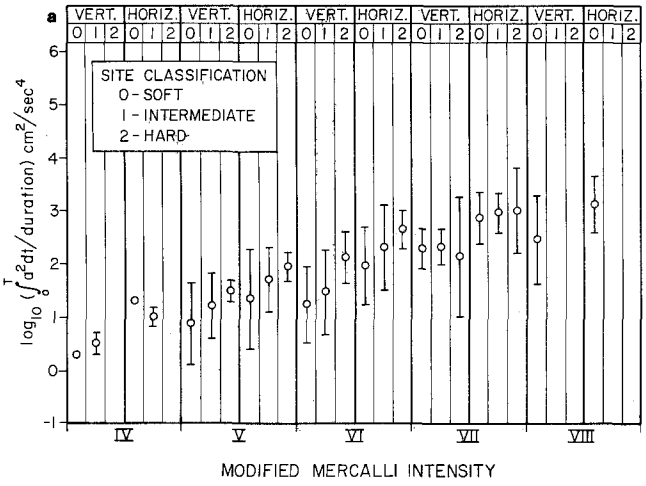

FIG. 9a. Mean values and standard deviations of the rate of growth of the integral $\int_0^T a^2\,dt$ for vertical and horizontal components at different site classifications and Modified Mercalli intensities.

CORRELATION OF THE RATE OF GROWTH OF STRONG GROUND MOTION WITH MAGNITUDE, EPICENTRAL DISTANCE, AND LOCAL SITE CONDITION

The rates of growth of strong-motion acceleration, velocity, and displacement as defined by equation (11) have been plotted for 181 vertical and 362 horizontal accelero-

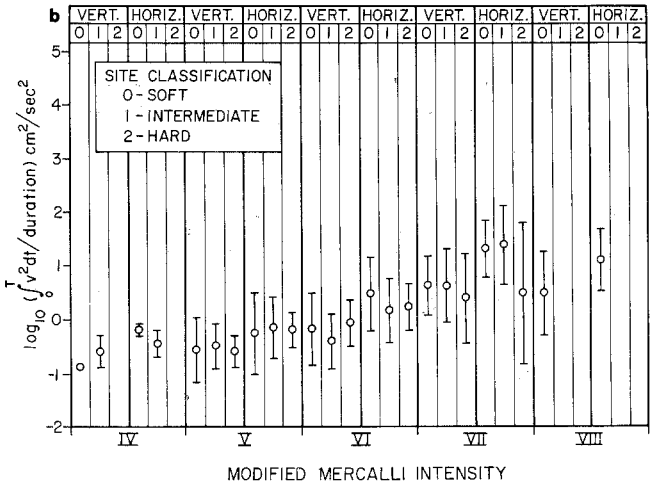

FIG. 9b. Mean values and standard deviations of the rate of growth of the integral $\int_0^T v^2 dt$ for vertical and horizontal components at different site classifications and Modified Mercalli intensities.

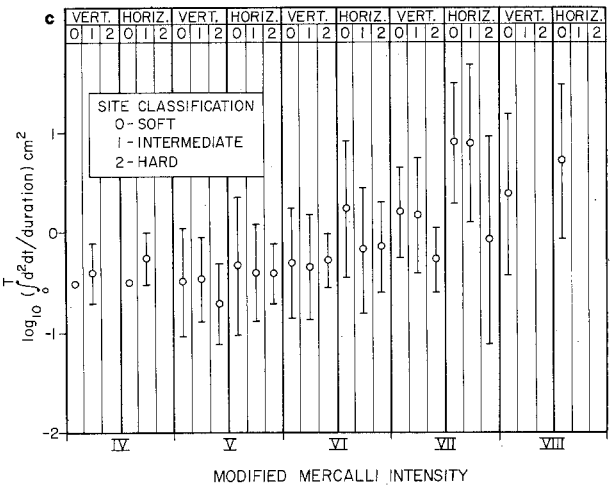

FIG. 9c. Mean values and standard deviations of the rate of growth of the integral $\int_0^T d^2 dt$ for vertical and horizontal components at different site classifications and Modified Mercalli intensities.

graph records in Figure 10 (a to f). Just as for the data in Figures 4 (a to f) and 7 (a to f), in Figure 10 (a to f) the scatter of observations seems to be quite large and no obvious trends with respect to magnitude or site conditions can be readily seen.

To find the average dependence of the rate of strong-motion acceleration, velocity, and displacement on the magnitude, M, site classification, s, and epicentral distance, Δ, we postulate the following linear model

$$\log_{10}\left\{\left[\int_0^T \begin{pmatrix} a^2 \\ v^2 \\ d^2 \end{pmatrix} dt\right]/\text{duration}\right\} = as + bM + c\log_{10}\Delta + d \pm \sigma \tag{31}$$

and assume that the standard deviation σ may be distance-dependent as follows

$$\sigma = A + B\log_{10}\Delta \pm \Sigma. \tag{32}$$

The coefficients a, b, c, d, A, and B and the standard deviation σ in (31) and Σ in (32) have been presented in Table 10. In agreement with Figure 9 (a, b, and c) the coefficients a in

TABLE 9

CORRELATION OF RATE OF ACCELERATION, VELOCITY, AND DISPLACEMENT WITH MODIFIED MERCALLI INTENSITY FOR DIFFERENT SITE CONDITIONS (0, 1, AND 2)

Intensity	Component	$\log_{10}[\int_0^T a^2 dt/\text{dur.}, (\text{cm}^2/\text{sec}^4)]$		$\log_{10}[\int_0^T v^2 dt/\text{dur.}, (\text{cm}^2/\text{sec}^2)]$		$\log_{10}[\int_0^T d^2 dt/\text{dur.}, (\text{cm}^2)]$		No. of Data
		Mean	Standard deviation	Mean	Standard deviation	Mean	Standard deviation	
III–0	Vertical	0.10	—	−0.70	—	−0.30	—	1
	Horizontal	0.80	—	−0.40	0.10	−0.20	0.10	2
III–1	Vertical							
	Horizontal							
III–2	Vertical	−1.10	—	−1.10	—	−0.70	—	1
	Horizontal	−1.20	0.10	−2.00	0.10	−2.10	—	2
IV–0	Vertical	0.30	—	−0.90	—	−0.50	—	1
	Horizontal	1.30	—	−0.20	0.10	−0.50	—	2
IV–1	Vertical	0.50	0.20	−0.60	0.30	−0.40	0.30	2
	Horizontal	1.00	0.17	−0.45	0.26	−0.25	0.26	4
IV–2	Vertical							
	Horizontal							
V–0	Vertical	0.89	0.77	−0.55	0.60	−0.48	0.54	17
	Horizontal	1.36	0.94	−0.25	0.75	−0.32	0.69	34
V–1	Vertical	1.22	0.61	−0.47	0.41	−0.46	0.42	15
	Horizontal	1.71	0.60	−0.15	0.56	−0.40	0.48	30
V–2	Vertical	1.50	0.20	−0.60	0.30	−0.70	0.40	2
	Horizontal	1.95	0.26	−0.20	0.33	−0.40	0.30	4
VI–0	Vertical	1.26	0.71	−0.17	0.66	−0.30	0.55	43
	Horizontal	1.96	0.73	0.48	0.68	0.24	0.68	86
VI–1	Vertical	1.49	0.80	−0.40	0.50	−0.34	0.52	16
	Horizontal	2.31	0.80	0.16	0.60	−0.16	0.63	32
VI–2	Vertical	2.13	0.49	−0.07	0.43	−0.27	0.27	7
	Horizontal	2.66	0.35	0.24	0.44	−0.13	0.45	14
VII–0	Vertical	2.30	0.38	0.64	0.55	0.21	0.45	50
	Horizontal	2.89	0.47	1.33	0.53	0.91	0.60	99*
VII–1	Vertical	2.32	0.33	0.63	0.69	0.18	0.57	21
	Horizontal	2.98	0.37	1.40	0.73	0.89	0.78	42
VII–2	Vertical	2.14	1.13	0.38	0.84	−0.26	0.32	5
	Horizontal	3.00	0.80	0.50	1.31	−0.06	1.04	10
VIII–0	Vertical	2.47	0.83	0.50	0.78	0.40	0.81	6
	Horizontal	3.12	0.53	1.13	0.58	0.73	0.77	12
VIII–1	Vertical							
	Horizontal							
VIII–2	Vertical							
	Horizontal							
X–0	Vertical							
	Horizontal							
X–1	Vertical							
	Horizontal							
X–2	Vertical	4.50	—	2.50	—	2.10	—	1
	Horizontal	4.90	—	2.90	0.20	1.90	0.60	2

*See footnote to Table 2.

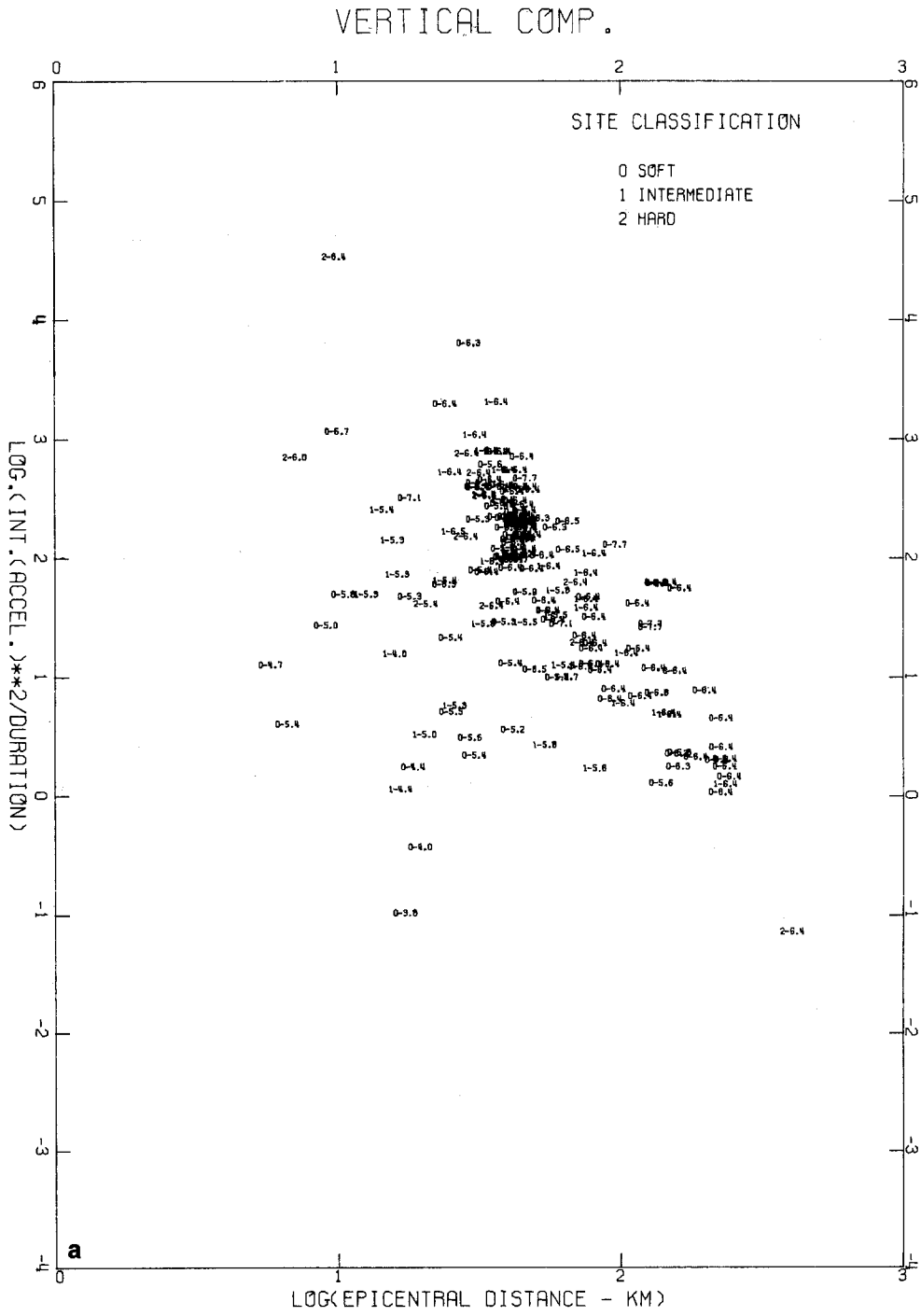

FIG. 10a. Correlation of the rate of growth of the integral $\int_0^T a^2 dt$, for vertical components, with site classification, magnitude, and epicentral distance.

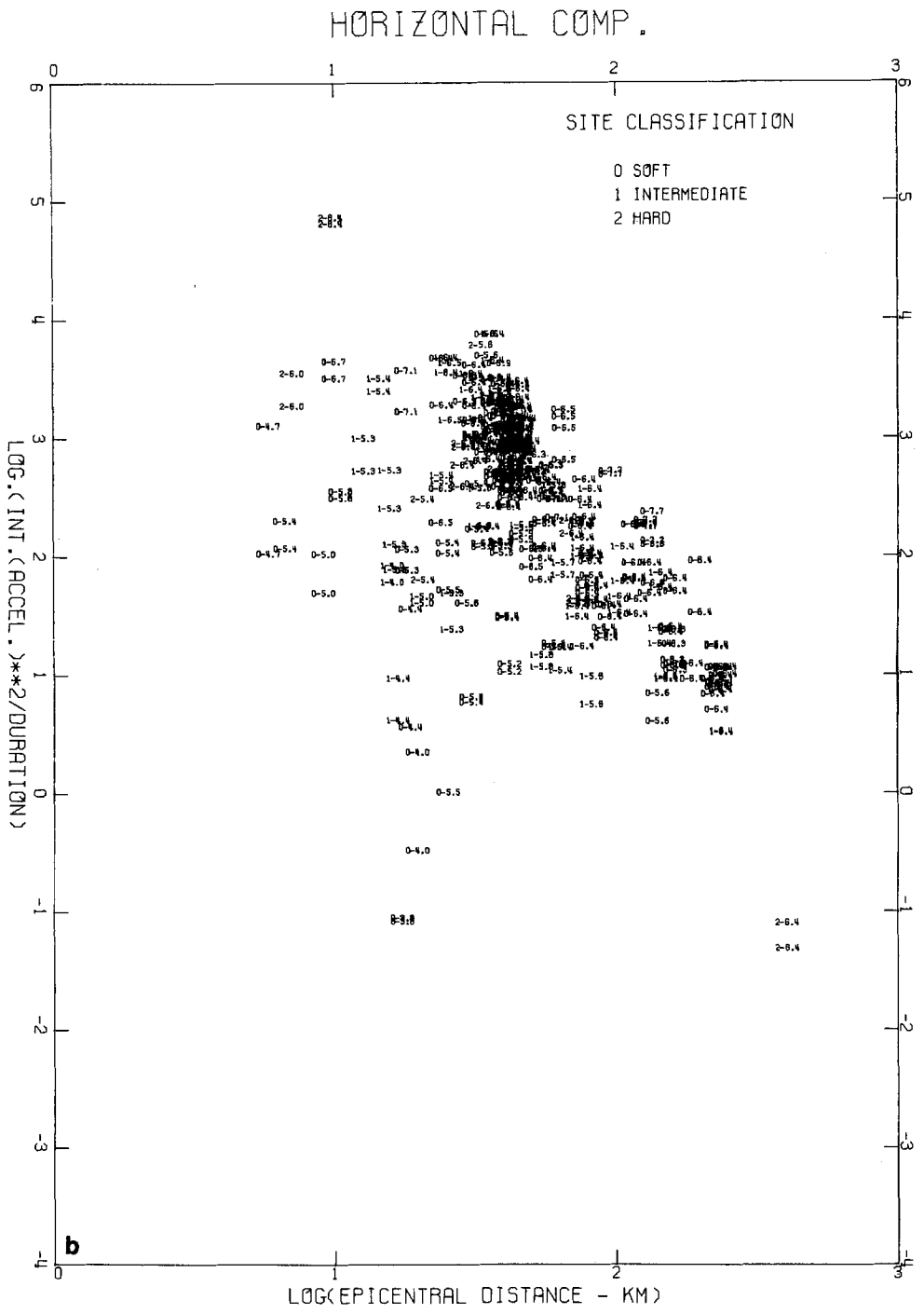

FIG. 10b. Correlation of the rate of growth of the integral $\int_0^T a^2\,dt$, for horizontal components, with site classification, magnitude, and epicentral distance.

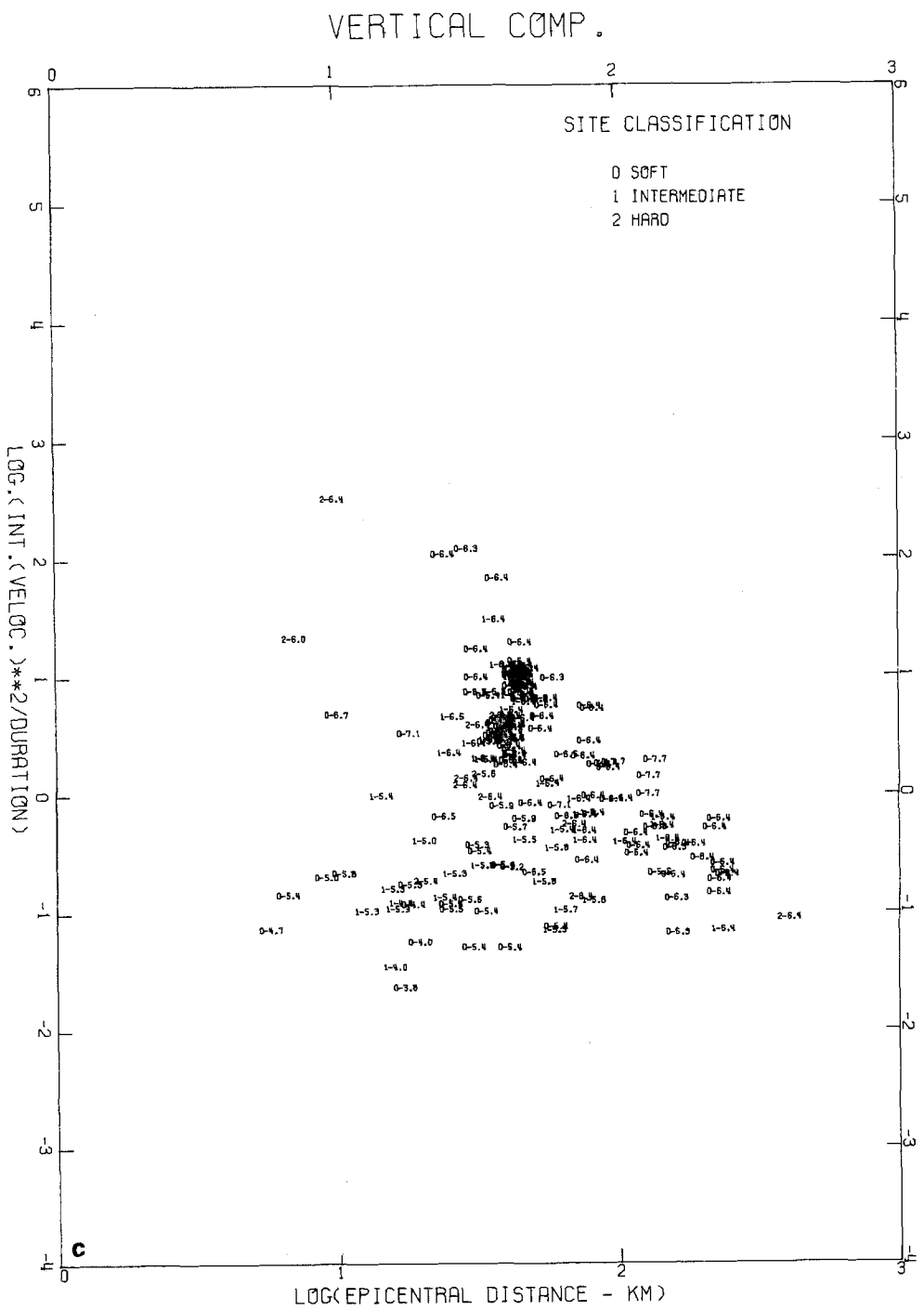

FIG. 10c. Correlation of the rate of growth of the integral $\int_0^T v^2 dt$, for vertical components, with site classification, magnitude, and epicentral distance.

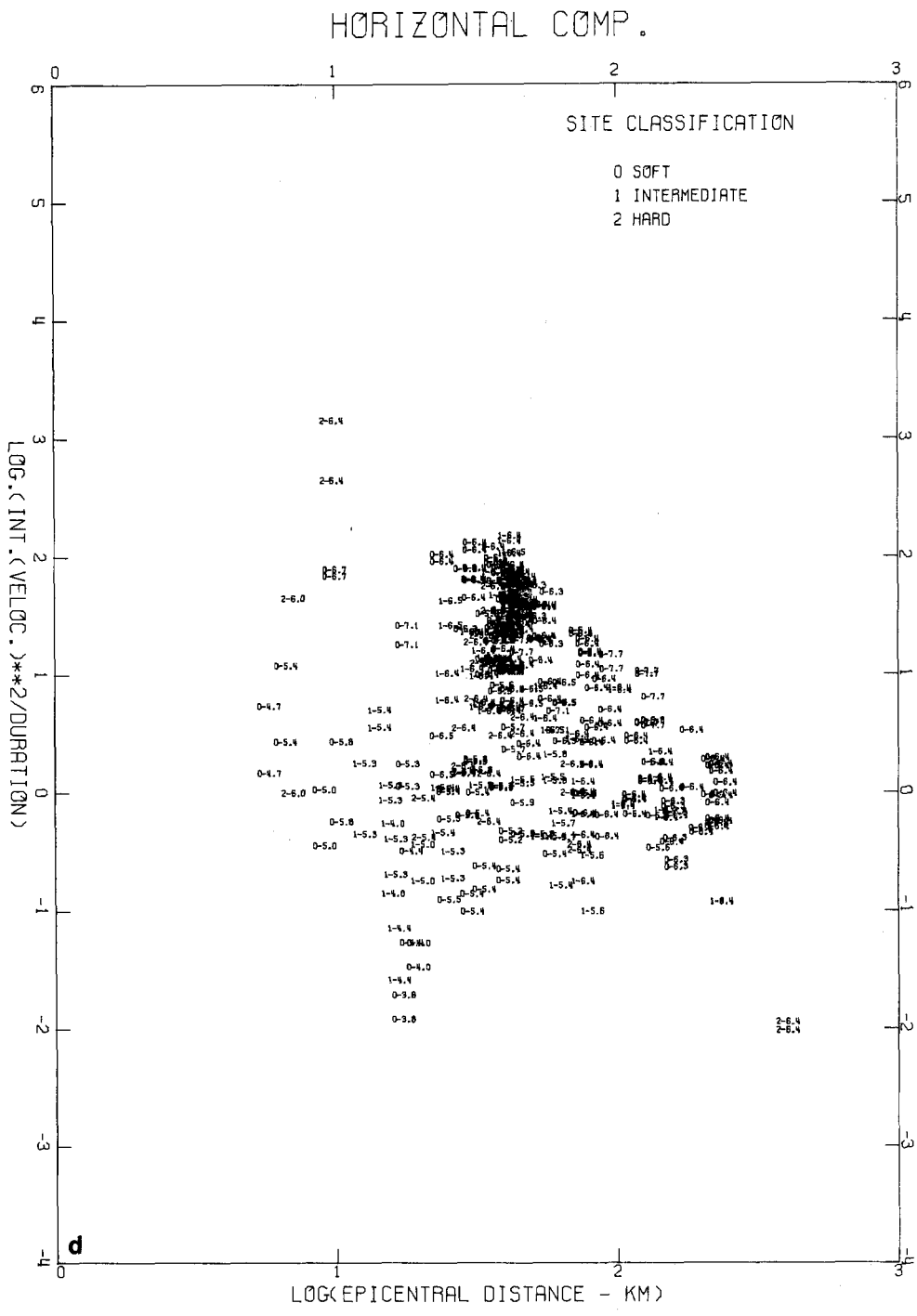

FIG. 10d. Correlation of the rate of growth of the integral $\int_0^T v^2 dt$, for horizontal components, with site classification, magnitude, and epicentral distance.

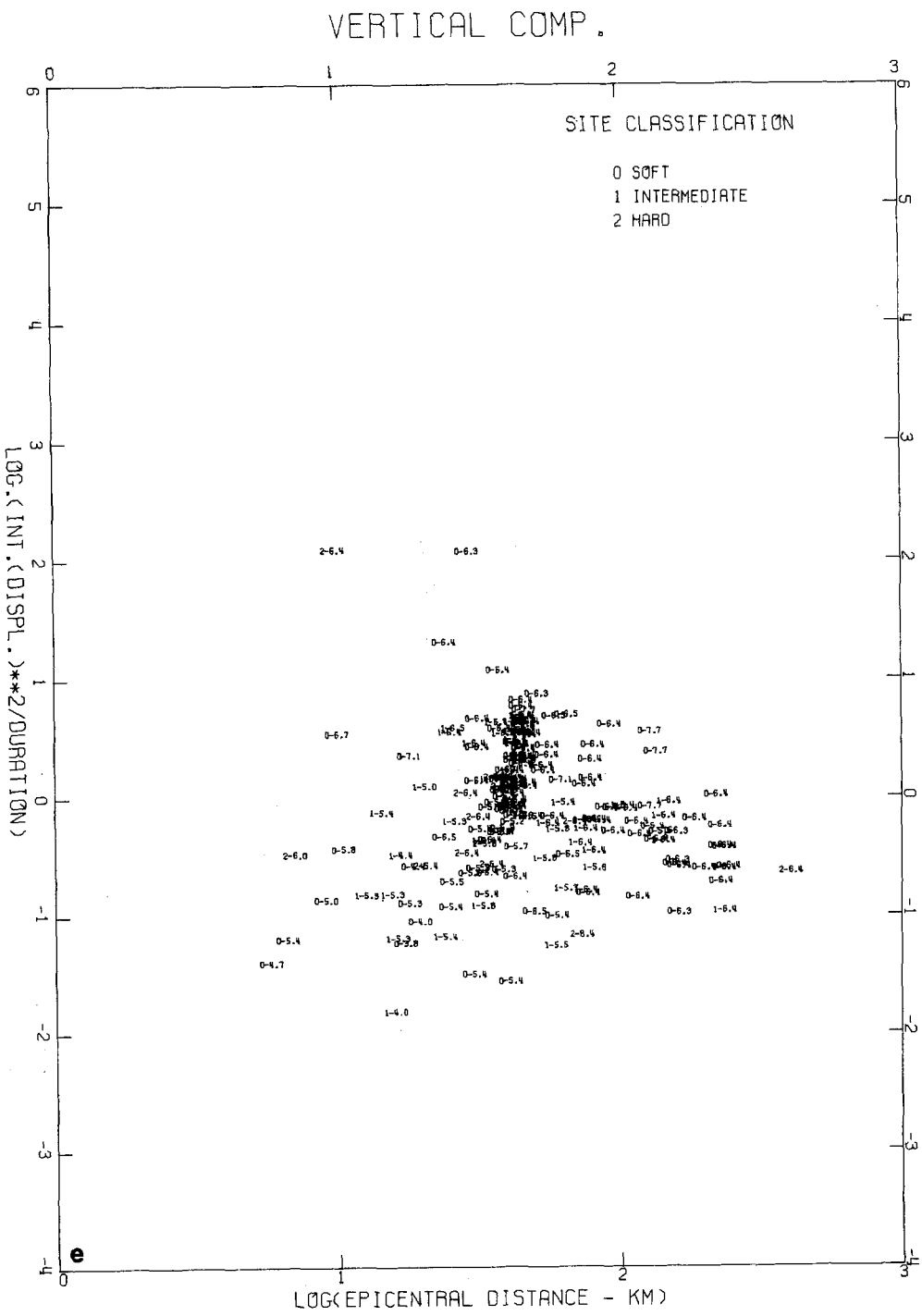

FIG. 10e. Correlation of the rate of growth of the integral $\int_0^T d^2 dt$, for vertical components, with site classification, magnitude, and epicentral distance.

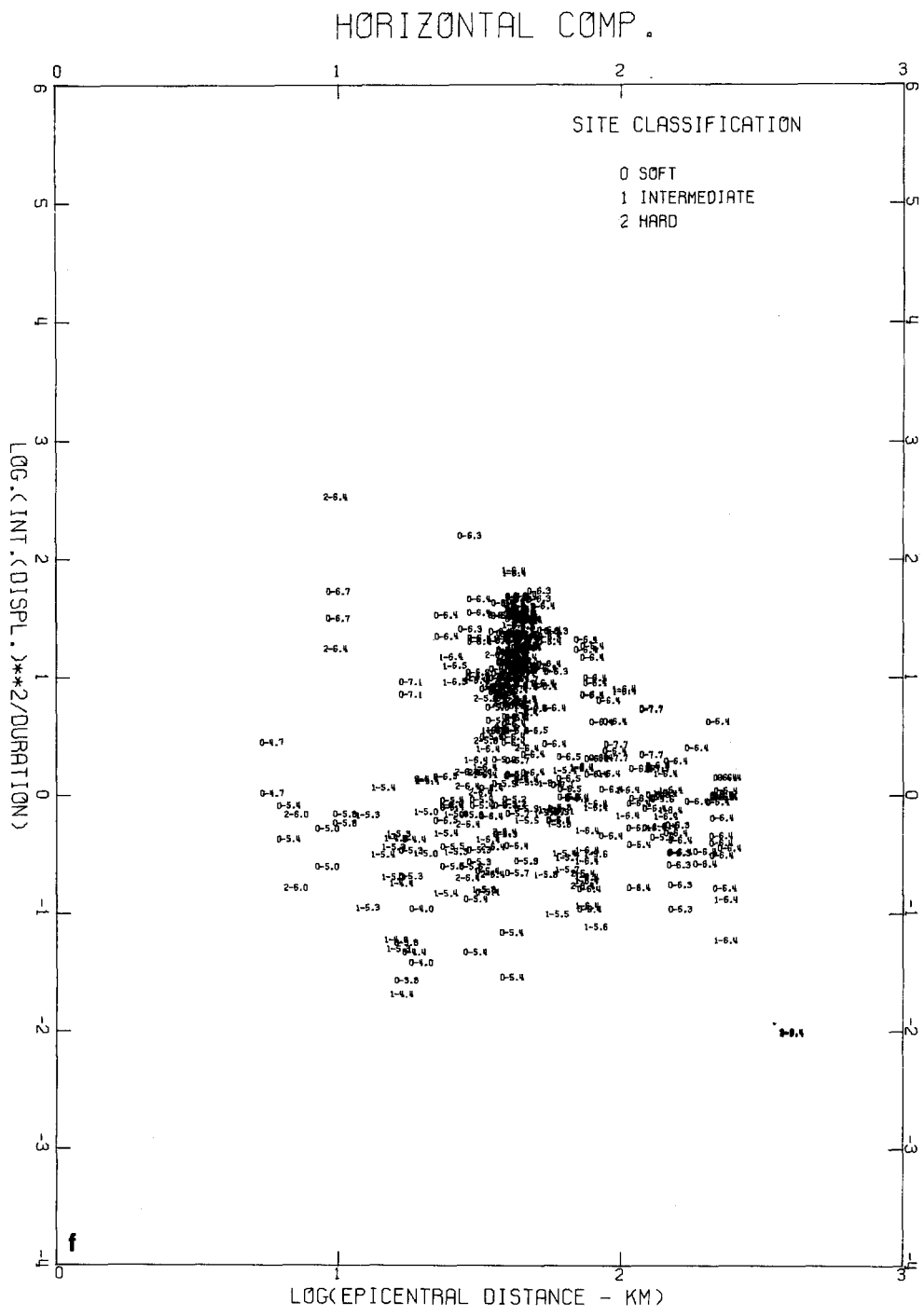

FIG. 10f. Correlation of the rate of growth of the integral $\int_0^T d^2 dt$, for horizontal components, with site classification, magnitude, and epicentral distance.

TABLE 10

COEFFICIENTS IN EQUATIONS

$$\log_{10}\left\{\int_0^T \begin{pmatrix} a^2 \\ v^2 \\ d^2 \end{pmatrix} dt/\text{duration}\right\} = as+bM+c\log_{10}\Delta+d\pm\sigma; \quad \sigma = A+B\log_{10}\Delta\pm\Sigma,^*$$

Component	a	b	c	d	σ	A	B	Σ	No. of data
				Acceleration					
Vertical	0.0913	1.07	−2.14	−1.36	0.548	0.873	−0.266	0.325	181
Horizontal	0.0471	1.10	−2.28	−0.661	0.565	0.866	−0.264	0.357	362
				Velocity					
Vertical	−0.0393	1.02	−1.30	−4.02	0.544	0.935	−0.306	0.320	181
Horizontal	−0.197	1.21	−1.70	−3.86	0.606	0.811	−0.188	0.337	362
				Displacement					
Vertical	−0.0562	0.700	−0.670	−3.29	0.481	0.845	−0.283	0.287	181
Horizontal	−0.250	0.973	−1.26	−3.44	0.634	0.759	−0.140	0.351	362

*For site classifications $s = 0$, 1 and 2, earthquake magnitude, M, and epicentral distance, Δ.

Table 10 indicate a tendency for acceleration growth rate to increase for "harder" sites, while the opposite trend is indicated for the rates of velocity and displacement. The effect of magnitude seems to be constant, whereas the decrease of the acceleration growth rate with distance is largest and that of displacement is smallest. This suggests that for the rate of strong ground motion the high-frequency attenuation plays a more important role than does the dispersion. The decrease of the standard deviation with distance appears to result from the similar decrease of the standard deviation of the integrals $\int_0^T a^2\,dt$, $\int_0^T v^2\,dt$, and $\int_0^T d^2\,dt$ (see Table 4) which is more prominent than the growth of the standard deviation of the duration with distance (Table 7).

CONCLUSIONS

The findings and conclusions of this paper depend in an important way on the particular definition of the duration of strong earthquake ground motion employed. We have here defined the duration of strong-motion acceleration to be that time interval during which the central 90 per cent of the contribution to the integral of the square of the acceleration takes place. We used the same definition for the duration of velocity and displacement. Although we made every attempt to use such a simple definition that can be related directly to the physical characteristics of response spectra, our results may be expected to give only the general and rough trends that characterize the duration of strong motion and should correspond to an upper bound for corresponding durations of specially chosen frequency bands inside the range of 0.07 to 25.0 Hz.

For low Modified Mercalli intensity (II and III) the average duration of strong-motion acceleration is about 45 sec and one standard deviation on either side of this mean is about 15 sec. With increasing intensity, duration decreases and becomes on the average 20 to 25 sec for intensity VIII. The average duration of strong-motion velocity and displacement also decreases in the same intensity interval from about 50 to 35 sec and from 40 to about 30 sec, respectively. The overall strong-motion amplitudes and spectral intensities which are proportional to the integrals $\int_0^T a^2\,dt$, $\int_0^T v^2\,dt$, and $\int_0^T d^2\,dt$, as well as

the rate of growth of these integrals, of course, increase with the increasing intensity. The increasing duration with decreasing intensity results from the dispersion with distance and the more pronounced scattering for the longer travel paths.

For the same Modified Mercalli intensity the average duration of strong-motion acceleration on a "soft" site is about twice longer than the duration at a "hard" site. Duration of strong-motion velocity and displacement indicates essentially the same trends. The overall spectral intensity of strong-motion acceleration is slightly higher on the "hard" basement rocks for intensities V and VI. This trend seems to disappear and is reversed for intensity VII. The spectral intensities of strong-motion velocity (proportional to $\int_0^T v^2\,dt$) and displacement (proportional to $\int_0^T d^2\,dt$) are consistently larger on "soft" alluvium than on the "hard" basement rocks by a factor ranging from about 2 to about 20.

Correlations of the duration of strong-motion acceleration, velocity, and displacement with site conditions, earthquake magnitude, and epicentral distance indicate that the average duration on a "soft" site is 5 to 6 sec longer than on "intermediate" site and about 10 to 12 sec longer than on a "hard" site. For each magnitude unit the duration increases by 2 (for acceleration) to about 5 (for displacement), while for every 10 km of distance it increases by about 1 to 1.5 sec.

Numerous linear regression relationships have been presented in this paper to describe more precisely, what is meant by "decreasing" or "increasing" of a function with respect to one or several of its arguments. Although such relationships are quite useful to detect the general trends in the data, and to bring out the most prominent factors that govern these trends, we would like to caution the reader not to use these simple relationships to compute the expected value of a function to which it applies. In using such simple relations there is always a danger of overlooking the quality of the fit or, more importantly, using the formulas in the range where they do not apply. Finally, it must be remembered that the functional forms of the formulas used in most cases cannot be justified on the physical basis of a problem but merely represent a simple and convenient mathematical form for the analysis. Instead, we suggest that having established the desired degree of conservatism in an analysis one should use the mean or the mean-plus-one standard deviation which are all presented in the different tables and figures.

The 188 accelerograph records used in this study, all recorded in the western United States, are barely adequate to suggest the possible average trends of the duration of strong-motion acceleration, velocity, and displacement and the related functionals for the Modified Mercalli intensity range between III and VIII and for the magnitude range between about 4 and 7.5. Since this data-set has been collected over the period of about 40 years, it is clear that it will be necessary to develop vigorous strong-motion data recording programs all over the world and to maintain these programs for many years before the number of the recorded accelerograms becomes adequate for more detailed and statistically sound analysis.

ACKNOWLEDGMENTS

We thank D. E. Hudson and J. E. Luco for critical reading of the manuscript and several useful comments.

This research has been supported by grants from the National Science Foundation and the Earthquake Research Affiliates Program at the California Institute of Technology.

REFERENCES

Arias, A. (1970). A measure of earthquake intensity in *Seismic Design of Nuclear Power Plants*, R. J. Hansen, Editor, The Mass. Inst. Tech. Press.

Bolt, B. A. (1973). Duration of Strong Ground Motion, World Conference on Earthquake Engineering, 5th Rome, 6-D, *Paper No. 292.*

Esteva, L. and E. Rosenblueth (1964) *Espectros de temblores a distancias moderadas y grandes, Bol. Soc. Mex. Ing. Sism.* **2**(1), 1–18.

Housner, G. W. (1952). *Intensity of Ground Motion During Strong Earthquakes*, Calif. Inst. of Tech., Earthquake Eng. Res. Lab., Pasadena.

Housner, G. W. (1965). Intensity of Ground Shaking Near the Causative Fault, *Proc. World Conf. Earthquake Eng., 3rd, New Zealand*, **3**, 94–109.

Housner, G. W. (1970). Strong ground motion, Chapter IV in *Earthquake Engineering*, R. L. Wiegel, Editor, Prentice Hall, Englewood Cliffs, N.J.

Hudson, D. E., A. G. Brady, M. D. Trifunac and A. Vijayaraghavan (1971). Strong-Motion Earthquake Accelerograms, Vol. II, Part A, Corrected Accelerograms and Integrated Velocity and Displacement Curves, Earthquake Engineering Research Lab., *EERL 71–57*, Calif. Inst. of Tech., Pasadena.

Husid, R. (1967). *Gravity Effects on the Earthquake Response of Yielding Structures*, Earthquake Eng. Res. Lab., Calif. Inst. of Tech., Pasadena.

Thatcher, W. and T. C. Hanks (1973). Source parameters of southern California earthquakes, *J. Geophys. Res.* **78**, 8547–8576.

Trifunac, M. D. and J. N. Brune (1970). Complexity of energy release during the Imperial Valley, California, earthquake of 1940, *Bull. Seism. Soc. Am.* **60**, 137–160.

Trifunac, M. D. (1971). Surface motion of a semi-cylindrical alluvial valley for incident plane *SH* waves, *Bull. Seism. Soc. Am.* **61**, 1739–1753.

Trifunac, M. D. (1972). Tectonic stress and source mechanism of the Imperial Valley, California, earthquake of 1940, *Bull. Seism. Soc. Am.* **62**, 1283–1302.

Trifunac, M. D., F. E. Udwadia, and A. G. Brady (1973). Analysis of errors in digitized strong-motion accelerograms, *Bull. Seism. Soc. Am.* **63**, 157–187.

Trifunac, M. D. (1973). A note on scattering of plane *SH* waves by a semi-cylindrical canyon, *Intern. J. Earthquake Eng. Struct. Dynamics* **1**, 267–281.

Trifunac, M. D. (1974). A three-dimensional dislocation model for the San Fernando, California, earthquake of February 9, 1971, *Bull. Seism. Soc. Am.* **64**, 149–172.

Trifunac, M. D. and A. G. Brady (1975). On the correlation of seismic intensity scales with the peaks of recorded strong ground motion, *Bull. Seism. Soc. Am.* **65**, 139–162.

Udwadia, F. E. and M. D. Trifunac (1973). Damped Fourier spectrum and response spectra, *Bull. Seism. Soc. Am.* **63**, 1775–1783.

Udwadia, F. E. and M. D. Trifunac (1974). Characterization of response spectra through the statistics of oscillator response, *Bull. Seism. Soc. Am.* **64**, 205–219.

Wong, H. L. and M. D. Trifunac (1974a). Scattering of plane *SH*-waves by a semi-elliptical canyon, *Intern. J. Earthquake Eng. Struct. Dynamics*, (in press).

Wong, H. L. and M. D. Trifunac (1974b). Surface motion of a semi-elliptical alluvial valley for incident plane *SH*-waves, *Bull. Seism. Soc. Am.* **64**, 1389–1408.

Wu, F. T. (1966). Lower Limit of the Total Energy of Earthquakes and Partitioning of Energy Among Seismic Waves, *Ph.D. Thesis*, Calif. Inst. of Tech., Pasadena.

Wyss, M. and J. N. Brune (1967). The Alaska earthquake of 28 March 1964; A complex multiple structure, *Bull. Seism. Soc. Am.* **57**, 1017–1023.

EARTHQUAKE ENGINEERING RESEARCH LABORATORY
CALIFORNIA INSTITUTE OF TECHNOLOGY
PASADENA, CALIFORNIA 91125

Manuscript received November 6, 1974